

Dynamic virtual ecosystems as a tool for detecting large-scale responses of biodiversity to environmental and land-use change

Claire L. Harris^{*1,4}, Christina A. Cobbold^{2,4}, Neil Brummitt^{3,4}, and Richard Reeve^{1,4}

¹ *Institute of Biodiversity, Animal Health and Comparative Medicine, College of Medical, Veterinary and Life Sciences, University of Glasgow, Glasgow, UK*

² *School of Mathematics and Statistics, University of Glasgow, Glasgow, UK*

³ *Natural History Museum, London, UK*

⁴ *Boyd Orr Centre for Population and Ecosystem Health, University of Glasgow, Glasgow, UK*

1 Abstract

In the face of biodiversity loss, we rely upon measures of diversity to describe the health of ecosystems and to direct policymakers and conservation efforts. However, there are many complexities in natural systems that can easily confound biodiversity measures, giving misleading interpretations of the system status and, as a result, there is yet to be a consistent framework by which to measure this biodiversity loss. Ecosystems are governed by dynamic processes, such as reproduction, dispersal and competition for resources, that both shape their biodiversity and how the system responds to change. Here, we incorporate these processes into simulations of habitat and environmental change, in order to understand how well we can identify signals of biodiversity loss against the background inherent variability these processes introduce. We developed a tool for Ecosystem Simulation through Integrated Species Trait-Environment Modelling (EcoSISTEM), which models on the species-level for several sizes of ecosystem, from small islands and patches through to entire regions, and several different types of habitat. We tested a suite of traditionally-used and new biodiversity measures on simulated ecosystems against a range of different scenarios of population decline, invasion and habitat loss. We found that the response of biodiversity measures was generally stronger in larger, more heterogeneous habitats than in smaller or homogeneous habitats. We were also able to detect signals of increasing homogenisation in climate change scenarios, which contradicted the signal of increased heterogeneity and distinctiveness through habitat loss.

2 Introduction

Untangling the response of ecological systems to disturbance is a complex challenge that has inspired ecologists for decades. Communities of plants and animals naturally

*Corresponding author. *Email address:* claire.harris@bioss.ac.uk

undergo disturbance throughout their lives, through climatic events such as fires and storms or biological pressures, such as predation and grazing (Dornelas, 2010). In fact, intermediate levels of these types of disturbance have long been thought to maximise species richness (Connell, 1978; Grime, 1973). More recently, the focus of disturbance ecology has shifted to anthropogenic impacts, with evidence of intensified pressure on ecosystems from an increasingly human-dominated planet (Dornelas, 2010). Long-term climate and land-use changes will increase the frequency and severity of shorter-term disturbance events on biological communities. These can act on populations directly, for example through increased mortality and decreased reproductive capacity, or they may impact on resources available to the species in the system. However, it is often difficult to untangle the impacts of disturbance from other confounding factors, such as the demographic fluctuations that populations naturally experience, or exactly which metric is used to calculate diversity (Santini *et al.*, 2016).

Although there is urgent need for large scale, species-focused modelling frameworks, those with greater geographical and taxonomic scope tend to lack important biological processes such as demographics, dispersal and competition (Urban *et al.*, 2016). Calls have already been made for more generalised models of diversity patterns, highlighting the need for a similar framework to the Intergovernmental Panel on Climate Change (IPCC), in which large scale climate models have been developed and are compared, as well as a system by which to monitor climate variables (Purves *et al.*, 2013). Such comparison with the IPCC is particularly apposite, considering that climate change, along with land-use change, is one of the biggest threats to biodiversity worldwide. Dynamic models like that of Harfoot *et al.* (2014), also known as the Madingley model, have already shown some success in replicating global patterns of diversity at the broad functional group scale. However, in the Madingley model, all terrestrial plants are reduced to a single group, autotrophs, with an associated total biomass. This lack of lower species-level data will be a hinderance when it comes to exploring the differential within-group responses to change and their measurement, a question at the forefront of modern ecology.

There have traditionally been three major approaches to modelling biological responses to climate change that range from species to community level (Hannah, 2014; Thuiller *et al.*, 2008). Species-level approaches are dominated by statistical correlations between current climate and species distributions to project forward under scenarios of environmental change (Keith *et al.*, 2008; Thuiller *et al.*, 2008). Due to their static nature, species distribution or environmental niche models (SDM/ENM) fail to account for important ecological processes that inform distributional changes such as competition, dispersal and evolution (Akçakaya *et al.*, 2006; Hannah, 2014; Pearson & Dawson, 2003; Thuiller *et al.*, 2008). Although often developed on a fine-scale, species by species level, which can be effectively extended to a global scope, SDMs would require the modelling of thousands of individual species to determine any community-level compositional changes in vegetation (Hannah, 2014). Furthermore, models that do not include any explicit biological mechanisms, particularly SDMs that are often based upon incomplete data, will predict new environments poorly. Despite this, the combined use of biological and climate records to construct an environmental niche for

species is a very valuable technique for parameterising larger-scale models.

Though there are many models that include whole-community dynamics, they often vary in geographic and taxonomic scale. Dynamic global vegetation models (DGVM), for example, simulate broad classes of plants as plant functional types (PFTs) with explicit mechanisms for fine-scale processes such as photosynthesis, growth and carbon cycling. DGVMs are now often coupled with Earth system models to incorporate feedbacks between environment and vegetation for improved climate predictions. One such model is the Joint UK Land and Environment Simulator (JULES), which originally classified plants in up to five functional groups; broad-leaved and needle-leaved trees, C3 and C4 grasses, and shrubs (Clark *et al.*, 2011). Coupled DGVMs are adept at answering questions about the direct and indirect effects of climate change and disturbance on different vegetation types. However, although improvements have been made to include more detailed functional groups in JULES (Harper *et al.*, 2016), such coarse ecological groups undoubtedly limit the use of DGVMs in conservation planning, or for exploring differential within-group responses to changing environments (Thuiller *et al.*, 2008). Equally, the models are primarily forced by detailed historical reconstructions and future climate predictions and they often lack direct input of anthropogenic disturbance, such as habitat loss or land-use change (Quillet *et al.*, 2010).

A popular alternative that operates with higher taxonomic information is the gap model, which simulates colonisation of gaps in the forest created when mature trees fall. Although they are dynamic, including processes such as growth and competition, gap models act at the species level to provide spatially-explicit predictions of changes in forest composition (Hannah, 2014; Thuiller *et al.*, 2008). Gap models are often limited to commercially important tree species and small areas, for which information on demographic and dispersal processes is more readily available. They also tend to be focused on trees in temperate regions, but have been extended in recent years to other systems such as grasslands, shrubs, and tropical trees (Fischer *et al.*, 2016; Moorcroft *et al.*, 2001). Due to the fact that gap models are individual-based, scaling them up to study the impact of climate change at regional or continental levels is computationally challenging, though there has been some progress for simulating tree dynamics in the Amazon rainforest, taking advantage of parallel processing and high performance computing (Fischer *et al.*, 2016; Shugart *et al.*, 2018). However, gap models of larger areas often rely upon aggregating species into functional groups, similar to their DGVM counterparts (Shugart *et al.*, 2018).

As with the biodiversity measures themselves, there is no single modelling approach that provides the functionality necessary to investigate biodiversity change at large scales to answer the questions we seek to address. However, there are several important dynamic processes in DGVM and gap models that should be considered. In particular, competition mechanisms vary across different model implementations, but most include some form of competition for light, water, space and nutrients like nitrogen (Quillet *et al.*, 2010). The vegetation model that drives JULES, Top-down Representation of Interactions between Foliage and Flora Including Dynamics (TRIFFID), approaches PFT competition through an adaptation of the Lotka-Volterra equations, by which there

are coefficients that determine the outcome of competition between different PFTs (Clark *et al.*, 2011; Cox, 2001). However, it is generally considered that competition by a resource pool rather than pre-determined outcomes is preferred for exploring responses to novel environments (Quillet *et al.*, 2010). In fact, theoretical approaches like the Maximum Entropy Theory of Ecology (METE) suggest that the allocation of energy and multiple resource parameters is what drives the structure of communities and allows more opportunities for rare species to thrive in their own niches (Harte & Newman, 2014).

Demographic processes such as reproduction, recruitment and mortality are also incorporated in DGVM and gap models, but are often uncoupled with the suitability of environment or availability of resources that drives competition. Dispersal, on the other hand, has traditionally not been explicitly modelled as plants are assumed to grow wherever conditions are suitable (Bugmann, 2001; Thuiller *et al.*, 2008). Several models now include a mechanism for dispersal, however (Engler & Guisan, 2009; Lexer & Hönninger, 2001). The importance of demography as a driver of stochasticity in ecosystems should not be underestimated, a point which is highlighted by many neutral theories of biodiversity. Given an ecosystem at equilibrium, simple birth-death-migration models can convincingly replicate the patterns of species diversity and abundance that we see in real systems like tropical forests (Hubbell, 1979, 2001). Beyond stochastic neutral changes in community composition, species competition for resources and suitability for their environments is a strong driver in their response to habitat and climate changes. All of these mechanisms are, therefore, critical when considering the dynamics of ecological communities. As a result, in order to thoroughly test the suitability of biodiversity measures at detecting trends in the presence of stochastic variability, a composite of all of these preceding approaches is needed. Such a model would need to operate at large scales for individual species and include mechanisms for biological processes such as competition and dispersal, sitting in the overlap between more traditional plant-climate models (Figure 1).

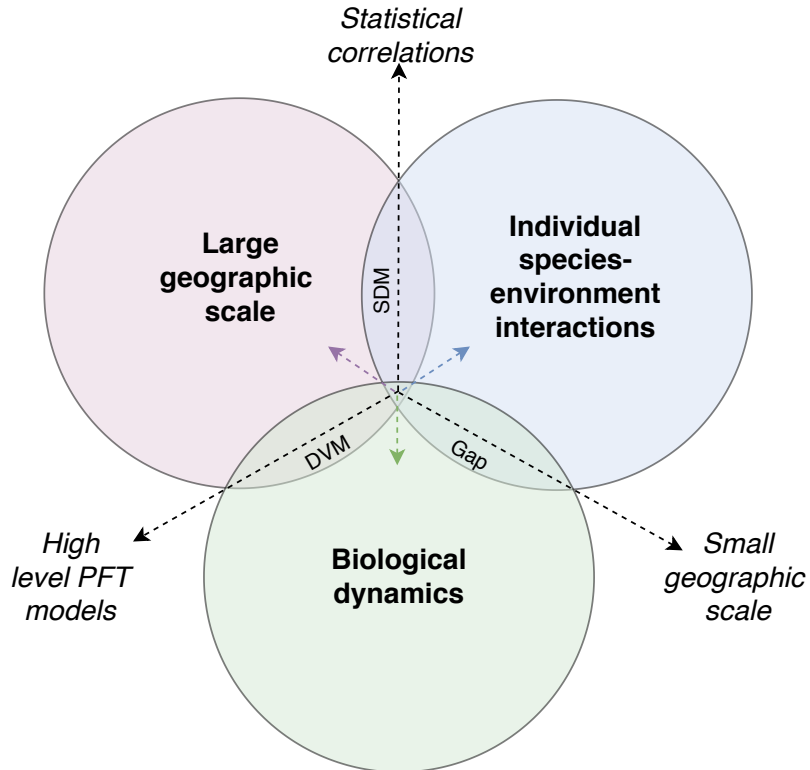


Figure 1: Schematic of three characteristics of different modelling approaches for the response of biodiversity to climate change, with examples of three predominant model types. Dynamic global vegetation models (DGVM) simulate several plant functional types undergoing biological processes, such as photosynthesis and carbon cycling. These have a whole community focus and can operate over large scales, but lack fine scale species information. Species distribution models (SDM) relate species observations with climate to make predictions about their current and future range. Compared to DGVMs, they are purely correlative models that include no biological mechanisms for species interaction. Finally, gap models simulate the growth of tree species to fill gaps in the forest and, whilst they include complex mechanisms for competition and growth, they are often focused on small regions and a limited number of species.

Here, we have developed exactly such a composite dynamic ecosystem model to fill this gap in the current modelling approaches, and explore its properties through idealised simulations of tropical plant ecosystems. Across the simulations we have created a range of different habitat types, from small-scale local patches with constant climates, to regional- or continental-scale areas with more complex climates. We used these different habitats to explore the underlying stochasticity in the system in the absence of external drivers of change and developed a range of biologically plausible scenarios of biodiversity loss, including that resulting from differing levels of future temperature change and habitat loss, in order to capture the response of a suite of

biodiversity measures and their ability to identify signals of change beyond the range of stochastic noise. In this case, we compared the power of traditional biodiversity measures against a new similarity-sensitive, effective number framework described by Reeve *et al.* (2016). Finally, we have added an additional layer of environmental variability in the form of seasonal temperature fluctuations into the simulations as a further test of the sensitivity of the different measures of biodiversity.

3 Model Development

3.1 General model structure

In order to investigate the effectiveness of diversity measures to quantify biodiversity in dynamic and changing systems, we created a tool for Ecosystem Simulation through Integrated Species Trait-Environment Modelling (EcoSISTEM) to describe a plant ecosystem. The system is built around several important related facets of community composition, including the trade-off between species' resource requirements and what is available in the environment in which they are found, and their fitness for that environment.

The 2D simulator landscape is discretised on a rectangular grid and we consider up to 10,000 species within the ecosystem, each with an abundance associated to each grid square as well as information on the niche preferences for each species, e.g. temperature ($^{\circ}\text{C}$), and the resource requirements—sunlight (kW) and water (mm). Also stored for each grid square are data on the habitat and resource availability for that location in the landscape. At each time step of the model (here, monthly), the habitat is updated, and species trait preference and resource requirements for the plants at that site are traded off against what is available. The match of species to their environment and resource needs impact reproduction and death rates. At the end of the step, seed dispersal takes place if reproduction has occurred.

We developed EcoSISTEM and created the underlying functionality as well as type system for this project. All of the code was written in Julia v1.1 (Besançon *et al.*, 2019; Bezanson *et al.*, 2017). In the following, we describe the different components of the model in a generalised format, and an overview of the model is represented by Figure 2.

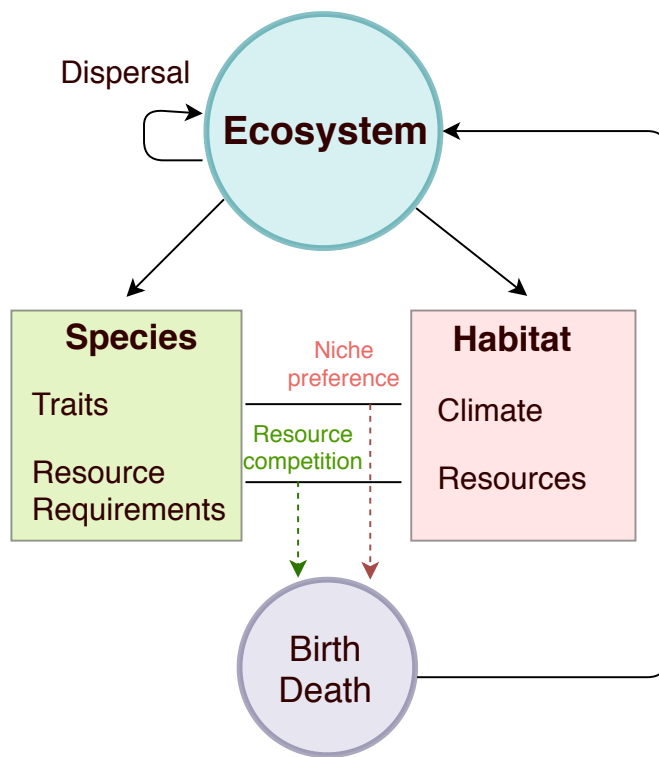


Figure 2: Overview of the ecosystem model in EcoSISTEM.

3.2 Properties

In the process of developing the model, we defined a series of properties and behaviours that the model should satisfy, including:

- Species are more abundant when more resources are available to them.
- Species' abundances scale with area and are invariant to grid size.
- Species with larger average dispersal distances can move further and faster across the landscape.

- Species have a competitive advantage when their niche preference is close to that of the climate.
- Specialist species with a narrow niche width have a competitive advantage over generalists with a broad niche width, for the same niche preference.
- Large numbers of species are sustained over large areas.

We considered these properties to be indicators that the model was performing in a biologically plausible manner, although this is not an exhaustive list. The results from this testing are presented in Section 5.1.

3.3 Population demographics

The dynamics of populations of any given species in the system can be described by equation 1 below. In it, the population at the next timestep, $t + \delta t$, at grid location X is a result of offspring dispersed and adults survived in the previous timestep t . The timestep δt can be altered but is set at a value of 1 month for these purposes.

$$pop(t + \delta t, X) = \underbrace{(pop(t, X) - Deaths(t, X))}_{\# \text{ Adults Survived}} + \underbrace{\sum_{Y=1}^N Births(t, Y) \times k(X, Y)}_{\# \text{ Offspring}} \quad (1)$$

where $pop(t, Z)$ is the population size of a species at time t in location Z , δt is the timestep, N is the number of grid locations in the ecosystem, $Births(t, Z)$ gives the number of births and $Deaths(t, Z)$ gives the number of deaths in location Z at time t . Finally, $k(V, W)$ gives the probability that a birth at source location W disperses to V to grow.

3.3.1 Births and deaths

The number of individuals of a particular species that are born or die in each timestep are drawn from a poisson and binomial distribution respectively, with the expected number of births per adult and probability of death as R_b and P_d , respectively (equations 2 and 3).

$$Births(t, X) \sim Poisson(pop(t, X) \times R_b(t, X)) \quad (2)$$

$$Deaths(t, X) \sim Binomial(pop(t, X), P_d(t, X)) \quad (3)$$

where $pop(t, X)$ is the size of the population of a species at time t and grid location X .

R_b and P_d depend on fixed expected birth and death rates, b and d , in a suitable environment with adequate resources, moderated by the availability of resource in the habitat and environmental suitability, B_e and D_e (see equations 4 and 5).

$$R_b(t, X) = b \times B_e(t, X) \times \delta t \quad (4)$$

$$P_d(t, X) = d \times D_e(t, X) \times \delta t \quad (5)$$

B_e and D_e act as penalty terms that depend on a species' raw resource requirements, as well as the ratio of total resource available, $K(X)$, to total resource used by all individuals in the grid square, $E(t, X)$. $K(X)$ does not change because we assume the resource is replenished at each time step. A species requiring more resources will give birth less often, but also live longer; a relationship present in many real-life species, including plants (Reich, 2001)(Figure 3). This process will also be modulated by how suited a species is to its environment, with those more mismatched facing decreased ability to reproduce and higher mortality through the adjusted resource requirement, ϵ' . These dynamics are captured in the equations 6 and 7.

$$B_e(t, X) = \underbrace{\left(\frac{\epsilon}{\bar{\epsilon}}\right)^{-\lambda}}_{\text{Penalty for resource requirement}} \times \underbrace{(\chi)^{-\tau}}_{\text{Penalty for mismatch to environment}} \times \underbrace{\min\left(\frac{K}{E(t, X)}, 1\right)}_{\text{Penalty for competition}} \quad (6)$$

$$D_e(t, X) = \underbrace{\left(\frac{\epsilon}{\bar{\epsilon}}\right)^{-\lambda}}_{\text{Boost for resource requirement}} \times \underbrace{(\chi)^{\tau}}_{\text{Boost for mismatch to environment}} \times \underbrace{\frac{E(t, X)}{K(X)}}_{\text{Boost for competition}} \quad (7)$$

where $\frac{\epsilon}{\bar{\epsilon}}$ denotes the normalised raw resource requirements of any particular species and χ is the resource requirement penalty for mismatch (Equations 10 and 11), $E(t, X)$ is the summed resource used by all individuals in grid cell X , i.e. $E(t, X) = \sum_{s=1}^S \epsilon_s \times \text{pop}_s(t, X)$, where subscript s denotes the species. Here, λ and τ are fixed parameters for the importance of resource requirements and the trait-environment relationship on birth-death. In the absence of data to fit these parameters, they were tuned for these simulations to give plausible results. Here $\lambda = 1$ and $\tau = 0.001$.

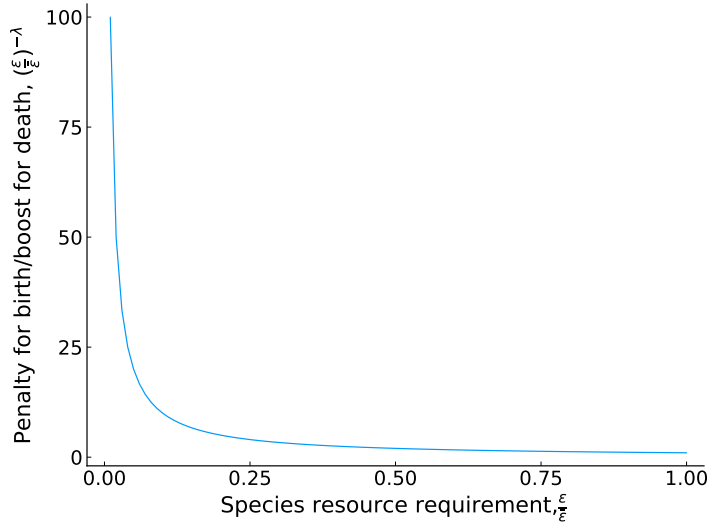


Figure 3: The relationship of species' resource requirements to birth and death processes. Species with larger requirements have a slower life cycle in that they will give birth less often and live longer than those with smaller requirements. λ is assumed to be 1.

It should also be noted that K and E are also normalised by the average resource requirement for all species $\bar{\epsilon}$, i.e. $\bar{\epsilon} = \frac{1}{S} \sum_{s=1}^S \epsilon_s$, to ensure that the values are comparable across different resources with different units. For births, the resource penalty is at least 1, where resource requirements and resource availability are exactly matched, so that there are only penalties and no advantages when there is more resource available than individuals to consume it. The need for such a term becomes evident when one considers extremely unsuitable conditions. Under these circumstances, the few remaining species in the model would otherwise get an enormous benefit from the availability of resources.

Following observations from METE, and considering the importance of both sunlight and water, we consider two resource systems. Here, equations 6 and 7 are modified as follows:

$$B_e(t, X) = \left(\frac{\epsilon_1}{\bar{\epsilon}_1} \times \frac{\epsilon_2}{\bar{\epsilon}_2} \right)^{-\lambda} \times (\chi_1 \times \chi_2)^{-\tau} \times \min \left(\frac{K_1(X)}{E_1(t, X)}, \frac{K_2(X)}{E_2(t, X)}, 1 \right) \quad (8)$$

$$D_e(t, X) = \left(\frac{\epsilon_1}{\bar{\epsilon}_1} \times \frac{\epsilon_2}{\bar{\epsilon}_2} \right)^{-\lambda} \times (\chi_1 \times \chi_2)^{\tau} \times \max \left(\frac{K_1(X)}{E_1(t, X)}, \frac{K_2(X)}{E_2(t, X)} \right) \quad (9)$$

with ϵ_1 , K_1 and E_1 normalised by the species average requirement for resource 1, $\bar{\epsilon}_1$ and similarly by $\bar{\epsilon}_2$ for ϵ_2 , K_2 and E_2 .

Lastly, we discuss the adjusted resource requirement, χ . We adjust the resource requirement of the species, ϵ , by the match of their niche preference to the current

environment, f (Equations 10 and 11) to penalise reproduction and increase mortality for species outside their natural habitats. Here, f is modelled as a Gaussian curve so that the penalty for being far away from the niche preference is normally distributed (De Blasio *et al.*, 2015), examples for which are given in Figure 4. However, this can be easily modified to consider alternative distributions. Here, we are considering a niche preference of temperature and examples of how species' temperature preferences translate to f can be found in Figure 4.

The niche mismatch penalty for a species, χ is described by the following:

$$\chi = \frac{\epsilon}{\bar{\epsilon} \times f(\bar{T}, T)} \quad (10)$$

where,

$$f(\bar{T}, T) = \frac{1}{\sqrt{2\pi\psi}} \times e^{-\frac{(\bar{T}-T)^2}{2\psi^2}} \quad (11)$$

and T is the current environment in a grid square, \bar{T} is the niche mean of the species, and ψ is the niche width (standard deviation) of the species. Note that this formula rewards species staying within their niche more if the niche is narrow, giving an advantage to specialists over generalists in this scenario.

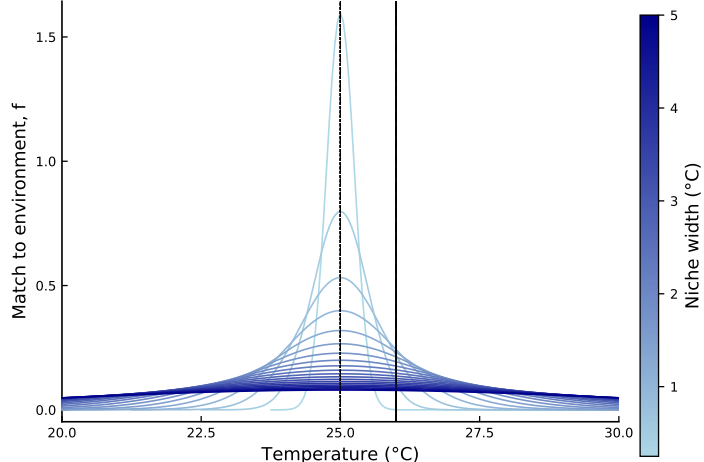


Figure 4: Match to the environment (f) for an example species with a temperature preference of 25°C. Here, we show the level of match across an environmental temperature range of 20 - 30°C for different niche widths (standard deviations).

3.3.2 Dispersal

Only individuals born in the current timestep are allowed to move, following the observation that for most plants, movement only occurs through seed dispersal. The probability of an individual dispersing to a grid square in the habitat is modelled as a Gaussian kernel and the probability of an individual from a species moving from anywhere in the source, Y , to destination, X , grid square, $k(X, Y)$ is described in

equation 12. An example of how dispersal is achieved in the model using area-to-area dispersal can be seen in Figure 5.

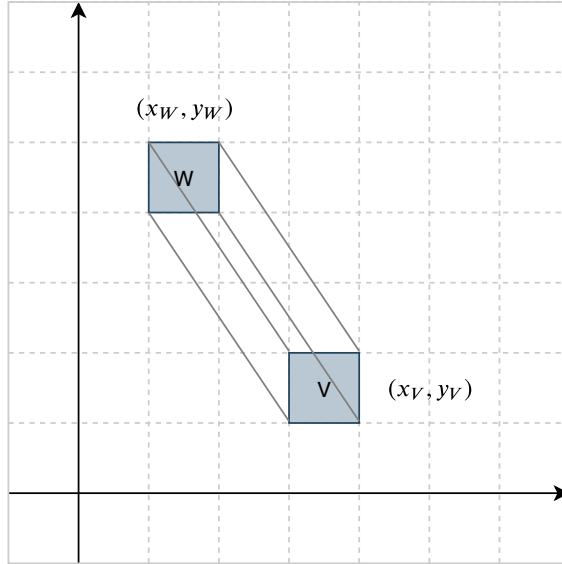


Figure 5: Diagram of area-to-area dispersal used in EcoSISTEM between source and destination grid squares, W and V , respectively. This diagram has been adapted from (Chipperfield *et al.*, 2011) in which the probability of moving from W to V is a result of integrating over all possible points in the source cell to all possible destination points in the destination cell.

$$k_{(V, W)} = \iiint_{\substack{V_x \in [x_V-1, x_V] \\ V_y \in [y_V-1, y_V] \\ W_x \in [x_W-1, x_W] \\ W_y \in [y_W-1, y_W]}} \frac{1}{\pi\theta^2} e^{-\frac{(V_x - V_y)^2 + (W_x - W_y)^2}{\theta^2}} dW_y dW_x dV_y dV_x \quad (12)$$

where $(x_V, y_V), (x_W, y_W)$ are the grid square indices of the destination and source grid square, respectively, 1 to n_V and 1 to n_W . θ is the width of the grid squares in standard deviations, or $\frac{\sigma}{\eta}$, where η is the size of the grid squares in the habitat and σ is the dispersal distance of a species.

The use of Gaussian dispersal kernels in the literature is contentious (Bullock *et al.*, 2017), but it remains the simplest option in the absence of direct information about dispersal, such as dispersal modes and seed size (see Section 4.2 for more details). For

comparison, we also test a fat-tailed 2Dt kernel (Clark *et al.*, 1999), as described by equation 13 (Section 4.2).

$$k_{(V, W)} = \iint \int_{\substack{V_x \in [(x_V-1), x_V] \\ V_y \in [(y_V-1), y_V] \\ W_x \in [(x_W-1), x_W] \\ W_y \in [(y_W-1), y_W]}} \frac{(b-1)}{\pi \theta^2} \times \left(1 + \frac{(V_x - V_y)^2 + (W_x - W_y)^2}{\theta^2} \right)^{-b} dW_y dW_x dV_y dV_x \quad (13)$$

where b determines the shape of the dispersal kernel's tail.

3.4 Virtual species

We simulated up to 10,000 virtual plant species across a range of different habitat types and scenarios of change to determine the ability of different diversity measures to see this change against the background stochastic variability. In order to give each species realistic characteristics, for each new ecosystem we generated a random phylogeny using the Phylo package in Julia (Reeve, 2019). Leaf area was modelled as an evolutionary trait along the tree using a Brownian motion model, under which the mean population trait value at the tips $\bar{\zeta}(\tau)$ of the tree is assumed to take a random walk from a starting value at the root, $\bar{\zeta}(0)$, using an evolutionary rate parameter, σ^2 , where τ is evolutionary time (Figure 6). Here, the value of $\bar{\zeta}(0)$ for leaf area was assumed to be 1.0m^2 and a σ^2 of $0.1\text{m}^2/\text{year}$.

3.4.1 Resource requirement, ϵ

The leaf area trait for each species was used to calculate the requirements of that species for the resource in the system, i.e. ϵ_s . Here, there are two resources; water and sunlight, for which we estimated the resource consumption to be 0.17kW and 192nm per individual per m^2 of leaf area, respectively. Solar energy consumption was calculated from WorldClim (Fick & Hijmans, 2017) records of average solar energy (kW/m^2) in comparable regions along the equator, and using the assumption that individual plants take up on average 1m^2 and that during photosynthesis, only around 38% of available light is absorbed by the plant (Amthor, 2010). Information on the ratio of water consumption to supply through precipitation is less available, although Good *et al.* (2017) calculate these values for a range of different plant biomes. Here we use a proportion of 44.5%, averaged across values from tropical lowland and montane areas and taking average water availability from WorldClim precipitation records in a similar manner (Fick & Hijmans, 2017).

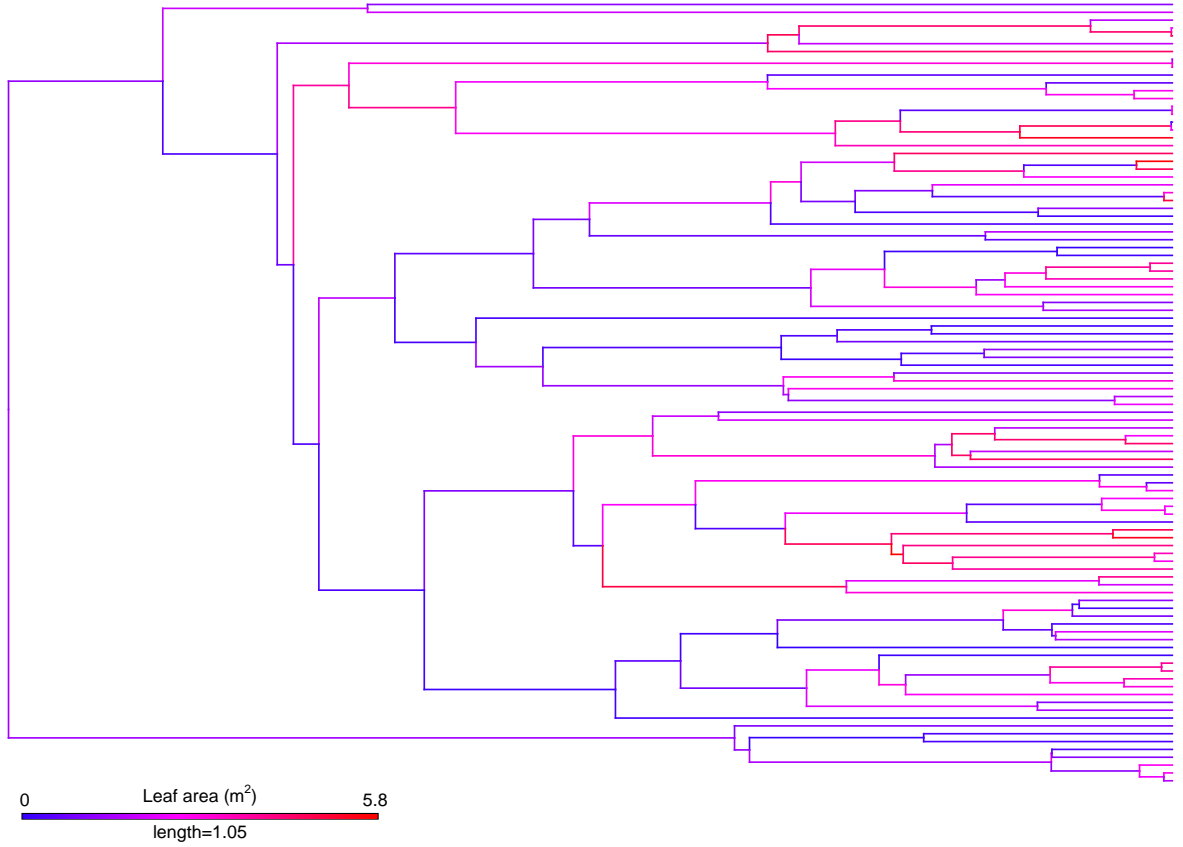


Figure 6: Example of continuous trait evolution of leaf area using Brownian motion. Here we simulate the average size of individuals in 100 virtual plant species, with a starting trait value of 1m^2 and evolutionary rate of $0.1\text{m}^2/\text{year}$.

3.4.2 Niche preference, \bar{T} & ψ

Each species was also assigned a niche preference. In this case, the habitat was comprised of different temperature profiles and so we assigned temperature mean, \bar{T} , along a gradient from minimum 20°C to maximum 30°C , and a niche width, ψ . This niche width was varied at random across the scenarios so that there were a range of specialists and generalists ($1\text{-}5^\circ\text{C}$).

4 Experimental Methods

4.1 Simulation environment

The simulation was run on habitats across three different scales; local, regional and continental (Table 1). Local habitats were divided into those that had some form of periodic boundary condition (“patches”) and those that were entirely isolated (“islands”). Habitats with larger areas, such as regions and continents could also support a greater number of species.

Table 1: Initial conditions for simulation experiments. Each simulation was run 100 times for each type of ecosystem change.

| Number of species | Area | Grid size | Habitat type | Boundary |
|-------------------|------------------------|-------------------|--------------|----------|
| 100 | 100km ² | 1km ² | Local | Torus |
| 100 | 100km ² | 1km ² | Local | Island |
| 1,000 | 10,000km ² | 10km ² | Regional | Cylinder |
| 10,000 | 200,000km ² | 80km ² | Continental | Torus |

For each of the habitats, we created a simplified tropical environment in which there is no seasonal variation in climate (except for the two temperature fluctuation scenarios) and derived suitable environmental parameters for the system using averaged historical data from WorldClim (Fick & Hijmans, 2017). we averaged monthly minimum and maximum temperatures, total precipitation and solar energy by taking bounding boxes around Northern Brazil, Gabon and Indonesia. Local habitats had a simple climate with a temperature that was constant across all grid squares, such as may be expected in very small areas, and were either islands or small patches within a larger area with dispersal across the x and y axes. Island habitats allowed no dispersal across either boundary, so that individuals could not move beyond the limits of the system. Larger regional and continental systems had more variability. For these, we employed different types of temperature gradient - linear and “peaked” respectively - as may be expected across larger landscape as temperature changes with altitude or latitude (Table 2). These temperatures ranged from 20°C to 30°C. All habitats had two types of resources, water and sunlight, for which we used values of 173.6 W/m² and 1.92×10^{-4} mm/m², which were approximately averages of the real life ecosystems for WorldClim. Regional habitats took the form of a cylinder, so that movement across the x boundary was allowed, but not the y , since it would result in discontinuities in temperature (see Table 2). In contrast, continental habitats took the form of a torus, so that species could move across both the x and y boundaries, enabling free movement in any direction and representing an effectively infinite plane.

Once species in the system equilibrated to the habitat type in question, by running the simulation for 10 years, we implemented several scenarios over the course of 50 years, including a neutral model in which no environmental change took place, invasion by a non-native species and directed change in habitat (see Table 3 for full details). The neutral scenario was used to measure stochasticity replicates when no other pressures are having an effect. Two types of invasive species were simulated - specialist and generalist. Specialist species had a narrow temperature preference for the specific area they were seeded, whereas generalists had a broader niche width and were subsequently seeded more widely (see Table 3 for more details). Habitat changes took the form of two of the major threats that plant species currently face, environmental and land-use change. Environmental change included projected global warming of 0.2°C per decade, the most likely scenario concluded by the IPCC (Intergovernmental Panel on Climate Change, 2018), although low to high projections ranged from 0.1°C to 0.3°C per decade. We also explored adding a seasonal fluctuation in temperature over the course of each year, as a standalone scenario as a reference to simulate a more temperate climate (though with otherwise tropical climates to reduce inter-model variability) and in combination with each of the projected temperature increases to simulate the effect of those changes to a temperate environment (Figure 7). Anthropogenic land-use changes included habitat loss at a rate of 10 per year, both random and clustered. For each replicate, the ecosystem population started identically for the each “ecosystem change” scenario, so that the change due to ecosystem change could be directly compared to the effect of the neutral scenario.

Table 2: EcoSiSTEM habitat types

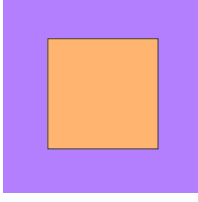
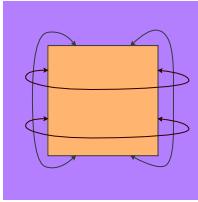
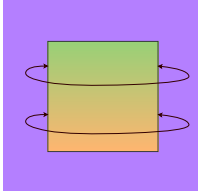
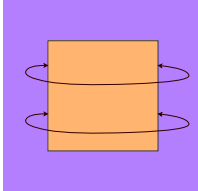
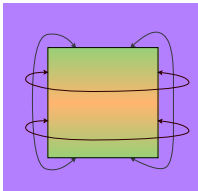
| Scale | Shape | Description |
|--|---|--|
| Local (100 km ²) |  | Small, homogenous island where no dispersal can take place across boundaries. |
| |  | Small, homogenous patch with dispersal across borders across both the x and y boundary, representing a patch in a large ecosystem. |
| Regional (10,000 km ²) |  | Larger area with dispersal across the x boundary, but not y . The gradient temperature pattern extended from cool areas at the top of the grid to warmer areas at the bottom, and represents landscape differences in temperature such as increasing altitude, representing a wide strip of land. |
| |  | Larger, homogenous area with dispersal across the x boundary, but not y . |
| Continental (200,000 km ²) |  | Largest area with dispersal across both the x and y boundary. Along the gradient the temperature peaked in the middle, with the top and bottom regions as the coolest, i.e. the poles, and thus represents latitudinal differences in temperature. This is a continental-scale model without concerns about edge effects due to size of the “continent”. |

Table 3: Types of ecosystem change.

| Type of change | Scenario | Description |
|----------------|-------------------------|---|
| No change | Neutral | Species experience uniform environments and levels of resources, so that their demographic fluctuation can be captured. |
| Competition | Generalist invasive | A generalist invasive species is introduced that grows at a rate of 1/50 of the average abundance per grid cell per species per year. This species is randomly seeded along the left-hand boundary and has the broadest niche width of all species. |
| | Specialist invasive | A specialist invasive species is introduced that grows at a rate of 1/50 of the other species abundances per year. This species is randomly seeded along the top boundary and is specially adapted for the warmest climates with the narrowest niche width of all species. |
| Environmental | Temperature increase | Each grid cell is increased in temperature by a rate of 0.1°C, 0.2°C or 0.3°C per decade, in line with anthropogenic global warming scenarios (IPCC, 2018). |
| | Temperature fluctuation | Seasonal fluctuation in temperature according to current global data. Each grid cell goes through a 12-month fluctuation from minimum to maximum temperature in line with what would be expected from global averages. |
| | Fluctuation + Increase | Both temperature increase and temperature fluctuation scenarios operating at the same time. |
| Land-use | Random habitat loss | At each timestep, a portion of the habitat is removed at a rate of 1/10 of the total habitat per year. The grid squares are chosen at random across the entire landscape and all individuals living in these grid squares are killed. |
| | Clustered habitat loss | At each timestep, a portion of the habitat is removed at a rate of 1/10 of the total habitat per year and all individuals living in these grid squares are killed. At each timestep a seed grid square is chosen at random from the landscape. After the initial step, portions of habitat are selected from neighbouring grid squares to those already lost so that habitat removal spreads out in clusters. |

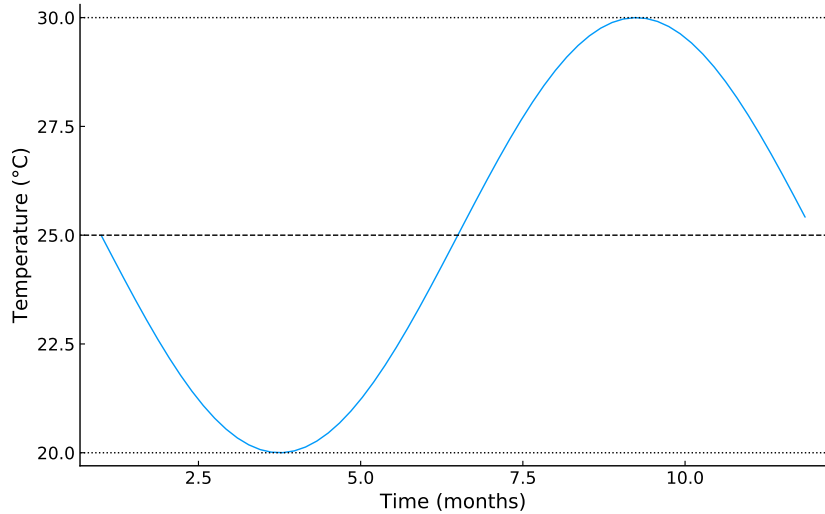


Figure 7: Example of the temperature fluctuation scenario, in which the environmental temperature of the ecosystem fluctuates $\pm 5^{\circ}\text{C}$ over the course of a year.

4.2 Biological assumptions

As with any ecological model, we have made several assumptions about the behaviour of the virtual ecosystem. First, we have specified that plant dispersal only takes place via seed dispersal, i.e. those that have just been born into the community disperse, as is observed in most plant species. There are a number of different ways a seed can be dispersed, including two commonly modelled mechanisms; anemochory and zochory. Under anemochory, or wind dispersal, a seed tends to fall closer to the plant than zochory, or animal-mediated dispersal (Thomson *et al.*, 2011). There is a great deal of speculation in the plant literature about which dispersal kernels most accurately capture plant seed dispersal, which differs greatly between plant types and dispersal mechanisms (Bullock *et al.*, 2017). Here we use a gaussian dispersal kernel, which concentrates offspring close to the parent plant. However, the model has the ability to be adapted to any form of dispersal kernel and has also been tested on a long-tailed 2Dt dispersal kernel (Clark *et al.*, 1999), which allows for some occasional long-distance dispersers.

Second, reproduction is modelled as a poisson process of germination rate per individual and current population size, making the assumption that time until the next production of seeds is exponentially distributed. Here, when we talk about each individual, we are really talking about one reproducing unit as there are many different methods by which plants reproduce. We took this to be a sensible approximation of the birth process, with an average number of germinations per adult plant per month that is determined by whether the plant is exposed to the correct environmental conditions to produce seed and whether they have enough resources to do so. Therefore, even though reproduction is a constant process throughout the simulation, plants are limited to windows of suitable conditions and will therefore be seasonal in their repro-

ductive patterns when seasonally fluctuating climate is introduced. In a similar way, we model death as a simple Bernouilli process for every individual at each timestep, which is regularly used for modelling survival processes (Caswell, 2001). The probability of death again depends on niche suitability and resource availability. The use of these distributions is a standard in demographic modelling (Chisholm *et al.*, 2014; Melbourne, 2012)

4.3 Parameterisation of the model

The simulations were run on a variety of different grid sizes and total areas ranging from 10 by 10 1km² grid squares on 100km² local patches, to 50 by 50 80km² grids on 200,000km², the range of which can be seen in Figure 8. We also explored several of the parameters in more detail, with smaller initial experiments to check the effect of varying demographic parameters on the outcomes of the simulations. These included birth, death and dispersal rates, as well as the type of kernel used to model dispersal, which were chosen from the relevant literature (see Table 4).

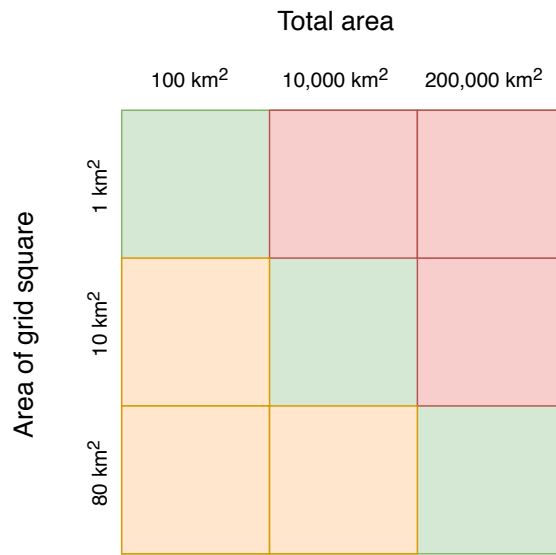


Figure 8: Illustration of the different grid sizes versus total area in simulation runs. Green identifies parameter combinations presented in these exploratory analyses, whereas red are computationally intractable with current cpu availability. Orange indicates parameter values that were computationally tractable, but not run here.

Table 4: Parameter values for EcoSiSTEM simulations

| Parameter name | Description | Value | Citation |
|----------------|--|---|----------------------------|
| P_b | Probability of birth | 0.001 – 0.15 per month | Marba <i>et al.</i> (2007) |
| P_d | Probability of death | 0.0015 – 2 per month | Marba <i>et al.</i> (2007) |
| σ | Average dispersal distance | 0.6 – 2.4 km | Clark <i>et al.</i> (1999) |
| K_1 | Total solar power available | 173.6 W/m ² | Fick & Hijmans (2017) |
| K_2 | Total water available | 1.92×10^{-4} mm/m ² | Fick & Hijmans (2017) |
| λ | Power of resource requirements on birth-death | 1 | - |
| τ | Power of trait-environment relationship on birth-death | 0.001 | - |
| \bar{T} | Optimum temperature for species | 20 - 30°C | - |
| ψ | Niche width | 1 - 5°C | - |
| δt | timestep | 1 month | - |

4.4 Initial conditions and runtime

All simulations were run for a “burn in” period of 10 years to allow species in the system to equilibrate and a further 50 years under a simulation scenario. Updates took place on a monthly basis and each experiment was repeated 100 times. We measured the response of biodiversity metrics to these scenarios every month. The contrasting measures are described in Tables 5 and 6. The measures in Table 6 were mostly chosen to be comparable to those in (Santini *et al.*, 2016), although functional indices are not included in this analysis. Those in Table 5 are a stand alone family of measures of alpha, beta and gamma diversity (Reeve *et al.*, 2016), for which we use the metacommunity measures for the purposes of this analysis. For the diversity framework measures, we have chosen a value of 1 for the parameter q , for simplicity of comparison to the more traditional measures and because it incorporates species abundances without weighting them more strongly towards rare species ($q \rightarrow 0$) or more common species ($q \rightarrow \infty$).

Table 5: Measures of alpha, beta, rho and gamma diversity from the Reeve *et al.* (2016) framework, in the form of ${}^qX^Z$ where X is the diversity measure in question (α, β, ρ or γ), Z is the similarity matrix and q is the viewpoint parameter. $Z = I$ assumes all species are equally distinct, as in Hill (1973). $P_{.j}$ is a vector of the relative abundances of all species in subcommunity j , p is a vector of the total relative abundances of species in the ecosystem, w is a vector of the number of individuals per subcommunity, $w_j = \sum_{i=1}^{n_{sc}} P_{ij}$ and $\bar{P}_{.j} = \frac{P_{.j}}{w_j}$, where $1 \leq i \leq n_{sp}$, $1 \leq j \leq n_{sc}$ for n_{sp} species and n_{sc} subcommunities.

| Type | Measure | Subcommunity | Metacommunity |
|------------|---|---|--|
| Alpha | Raw alpha | ${}^q\alpha_j^Z = M_{1-q}(\bar{P}_{.j}, \frac{1}{ZP_{.j}})$ | ${}^qA^Z = M_{1-q}(w, {}^q\alpha^Z)$ |
| | Normalised alpha | ${}^q\bar{\alpha}_j^Z = M_{1-q}(\bar{P}_{.j}, \frac{1}{Z\bar{P}_{.j}})$ | ${}^q\bar{A}^Z = M_{1-q}(w, {}^q\bar{\alpha}^Z)$ |
| Beta | Raw rho | ${}^q\rho_j^Z = M_{1-q}\left(\bar{P}_{.j}, \frac{\bar{Z}p}{ZP_{.j}}\right)$ | ${}^qR^Z = M_{1-q}(w, {}^q\rho^Z)$ |
| | Raw beta | ${}^q\beta_j^Z = \frac{1}{{}^q\rho_j^Z}$ | ${}^qB^Z = M_{1-q}(w, {}^q\beta^Z)$ |
| | Normalised rho | ${}^q\bar{\rho}_j^Z = M_{1-q}\left(\bar{P}_{.j}, \frac{Zp}{Z\bar{P}_{.j}}\right)$ | ${}^q\bar{R}^Z = M_{1-q}(w, {}^q\bar{\rho}^Z)$ |
| Gamma | Normalised beta | ${}^q\bar{\beta}_j^Z = \frac{1}{{}^q\bar{\rho}_j^Z}$ | ${}^q\bar{B}^Z = M_{1-q}(w, {}^q\bar{\beta}^Z)$ |
| | Gamma | ${}^q\gamma_j^Z = M_{1-q}(\bar{P}_{.j}, \frac{1}{Zp})$ | ${}^qG^Z = M_{1-q}(w, {}^q\gamma^Z)$ |
| Power mean | $M_r(u, x) = \begin{cases} (\sum_{i=1}^n u_i \times x_i^r)^{\frac{1}{r}}, & r \neq 0 \\ \prod_{i=1}^n x_i^{u_i}, & r = 0 \end{cases}$ | | |

Table 6: Selection of traditionally used biodiversity metrics and their relation to the Reeve *et al.* (2016) framework, where $p_i(t)$ is the abundance of species i and n_{sp} is the number of species, L_k is the length of branch k in the phylogeny where N_b is the number of branches.

| Measure | Equation | Reference | Reeve <i>et al.</i> (2016) equivalent |
|-------------------------------|---|-----------------|---|
| Species richness [‡] | $\sum_{i=1}^{n_{sp}} \mathbb{1}p_i(t) > 0$ | - | ${}^0\bar{\alpha}^I$ or ${}^0G^I$ |
| Shannon entropy | $-\sum_{i=1}^{n_{sp}} p_i(t) \ln p_i(t)$ $i : p_i(t) > 0$ | Shannon (1948) | $\ln({}^1\bar{\alpha}^I)$ or $\ln({}^1G^I)$ |
| Simpson index | $1 - \sum_{i=1}^{n_{sp}} p_i(t)^2$ | Simpson (1949) | $\frac{1}{2\bar{\alpha}^I}$ or $\frac{1}{2G^I}$ |
| Arithmetic mean abundance | $\frac{\sum_{i=1}^{n_{sp}} p_i(t)}{n_{sp}}$ | - | - |
| Geometric mean abundance | $\prod_{i=1}^{n_{sp}} 1 + p_i(t)^{\frac{1}{n_{sp}}}$ | - | - |
| Sørenson similarity | $1 - \frac{\sum_{i=1}^{n_{sp}} p_i(t-1) - p_i(t) }{\sum_{i=1}^{n_{sp}} p_i(t-1) + p_i(t) }$ | Sørensen (1948) | - |
| Faith's PD* | $\sum_{k=1}^{N_b} L_k$ | Faith (1992) | ${}^0G^Z \times \frac{\sum_{k=1}^{N_b} L_k}{N_b}$ |

* Faith's PD is the phylogenetic equivalent of richness and here Z is a branch-based similarity matrix (See Leinster & Cobbold (2012) for more details).

‡ $\mathbb{1}p_i(t) > 0$ is an indicator variable, 1 when $p_i(t) > 0$, 0 when $p_i(t) = 0$

We subtracted the results of the neutral scenario, in which no environmental change took place, from the rest of the scenarios and calculated the slope of change from linear models. This represents the extent of biodiversity change beyond neutral stochastic variations in the underlying system. In each of the following results, we compared the raw slope values of the neutral scenario, for a sense of “within run” variability, to those of a different run, for “between run” variability. Then, each of the subsequent scenarios with the same starting populations, as described in Section 3, are the slope of change following neutral correction, which can be compared to the between run variability.

In the exploration of parameter space, we also used an initial simulation built for just 100 species over a smaller landscape. We varied birth, death and dispersal rate along a gradient of values observed in plant systems, which had an effect on the ability

of the system to cope with the scenario of change. For example, those with higher birth rates, on average, experienced less drastic declines in abundance and evenness. However, the following experiments include species with a range of parameter values from the literature (Table 4).

5 Results

5.1 Model Testing

Throughout the development of the model in Section 3, experiments were run in order to confirm appropriate dynamics. Firstly, we confirmed that abundance depended upon the amount of available resource (Figure 9). Here, we simulated an island ecosystem with two resources, water and sunlight, each on a gradient West to East and South to North, respectively. Abundance increased in squares with greater amounts of water and sunlight, with some edge effects. Next, we investigated the relationship between abundance and area size. As expected, ecosystems with greater areas could support more individuals (Figure 10), and these abundances were invariant to the resolution of the grid (Figure 11). However, at larger grid sizes, abundances may be limited by a lack of dispersal. We also verified that dispersal functioned correctly, so that species with larger average dispersal distances moved further and faster through the landscape. Figure 12 shows the overall abundance of an island populated with two species at opposite extremes of the ecosystem after ten years of simulation. The species moved faster and further into the unpopulated island centre when they had higher average dispersal distances, though again with some edge effects.

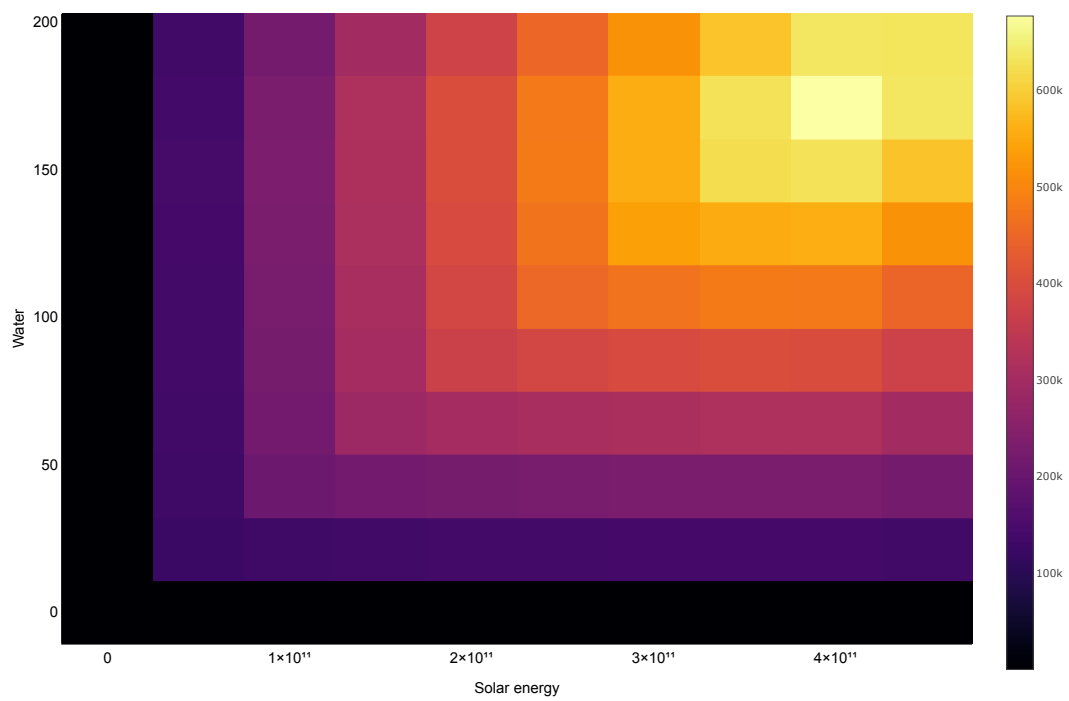


Figure 9: Total abundance of 100 species in an *island* ecosystem, with varying resources of water and solar energy across the grid.

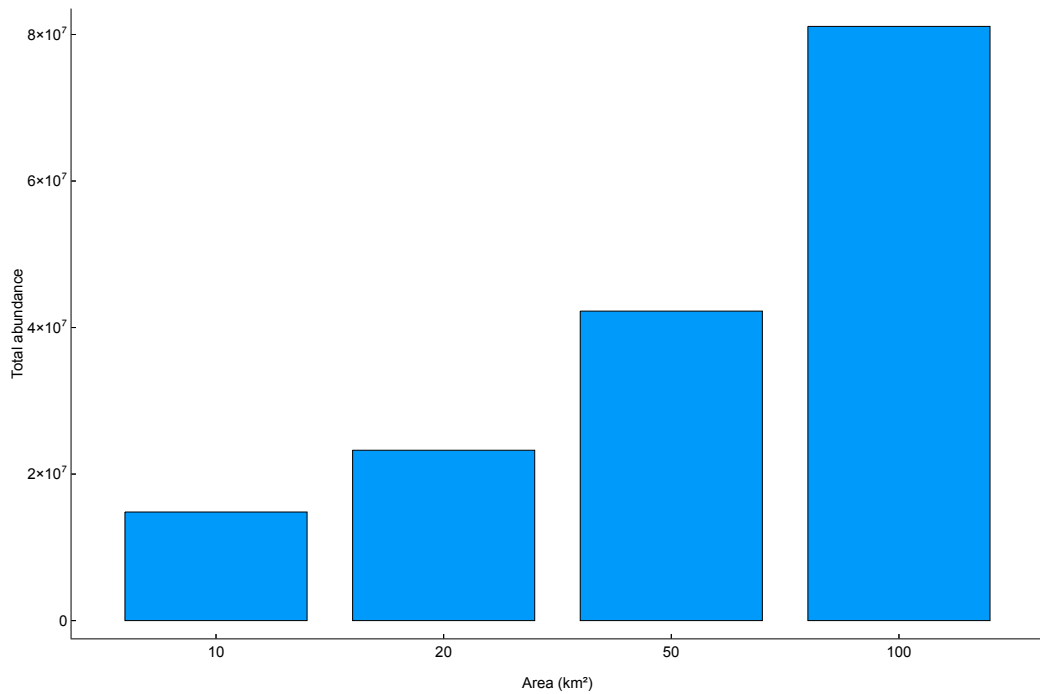


Figure 10: Total abundance of 100 species in *patch* ecosystems, with increasing area size.

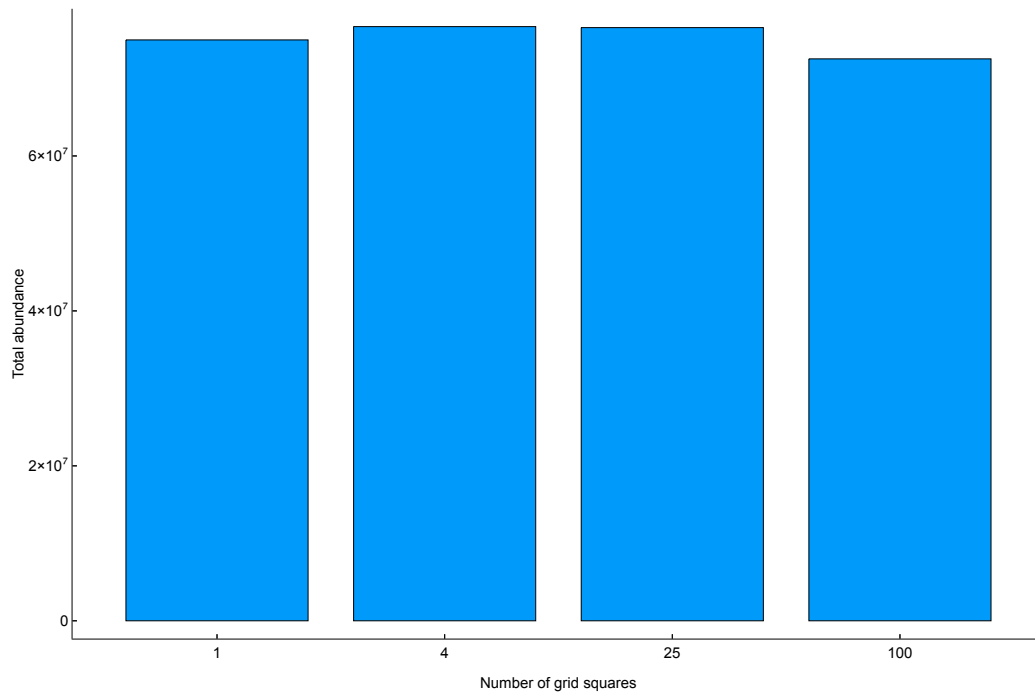


Figure 11: Total abundance of 100 species in *patch* ecosystems, with increasing grid square resolution.

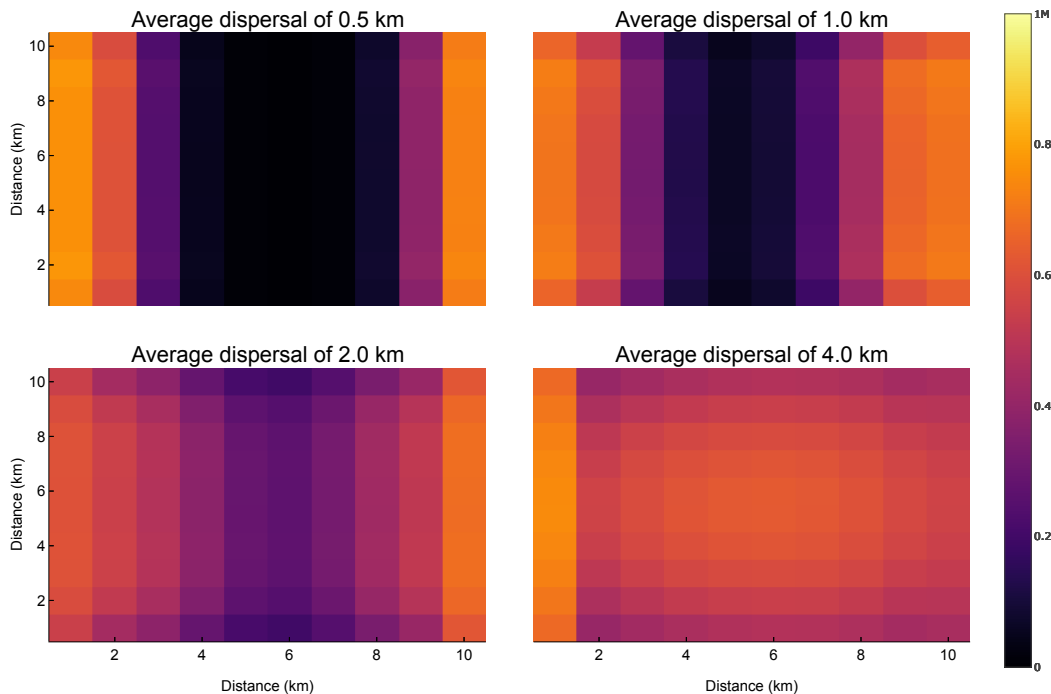


Figure 12: Total abundance of two species in *island* ecosystems after 10 years of simulation, with species populated at opposite sides of the island. Those with higher dispersal distances moved further away from their starting populations at a faster rate.

Considering individual species, we also tested that species' niche preferences and widths functioned correctly. On a patch sized ecosystem, across 100km^2 with 100 species and a homogeneous climate of 25°C , we explored the abundance of species given different niche preferences, with all other parameters kept equal. We found that species with niche preference nearer to the 25°C optimum were more abundant, when all species were given the same niche widths (Figure 13). Additionally, when all species had a preference for the 25°C climate and a range of niche widths, those with broader niche widths (generalists) were less abundant than species with narrow (specialists) (Figure 14). This drop in abundance is anticipated given the decline in species match to environment as niche width moved from 0 to 1°C in Figure 4. If the temperature in the ecosystem was then increased by 1°C , those with the narrowest niches went extinct, and the generalists became more abundant (Figure 15), with a slight preference for those with a niche width of around 1°C as we would expect from Figure 4.

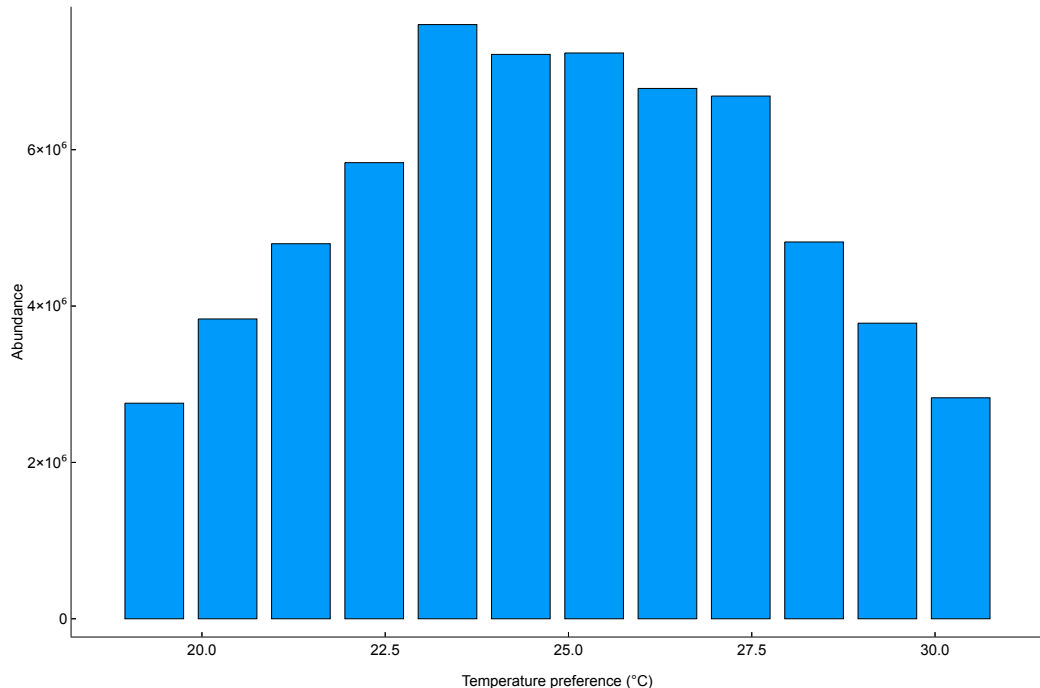


Figure 13: Abundance of species with different temperature preference across 100km^2 patch ecosystem with 100 species and a homogeneous climate of 25°C .

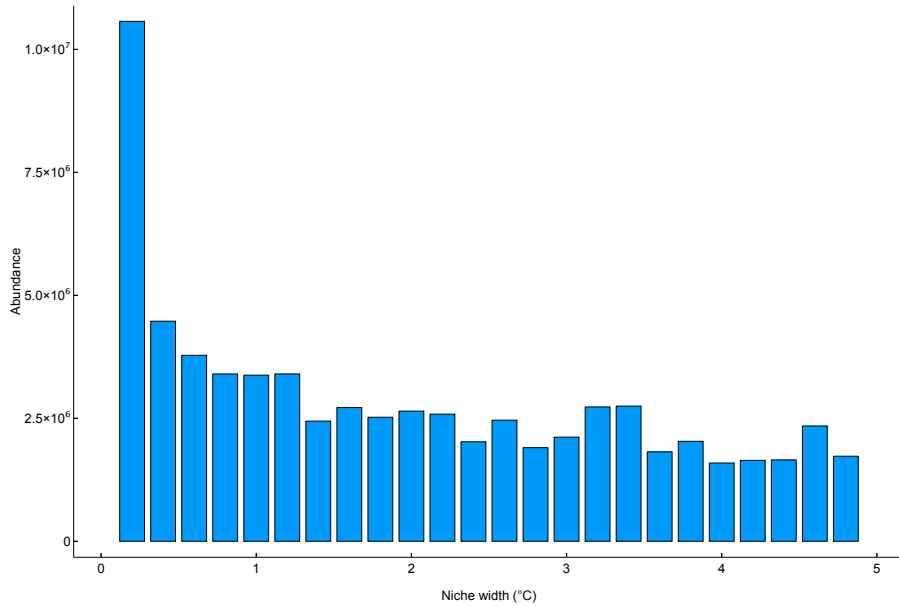


Figure 14: Abundance of species with different niche widths and a temperature preference for 25°C, across 100km² *patch* ecosystem with 100 species and a homogeneous climate of 25°C.

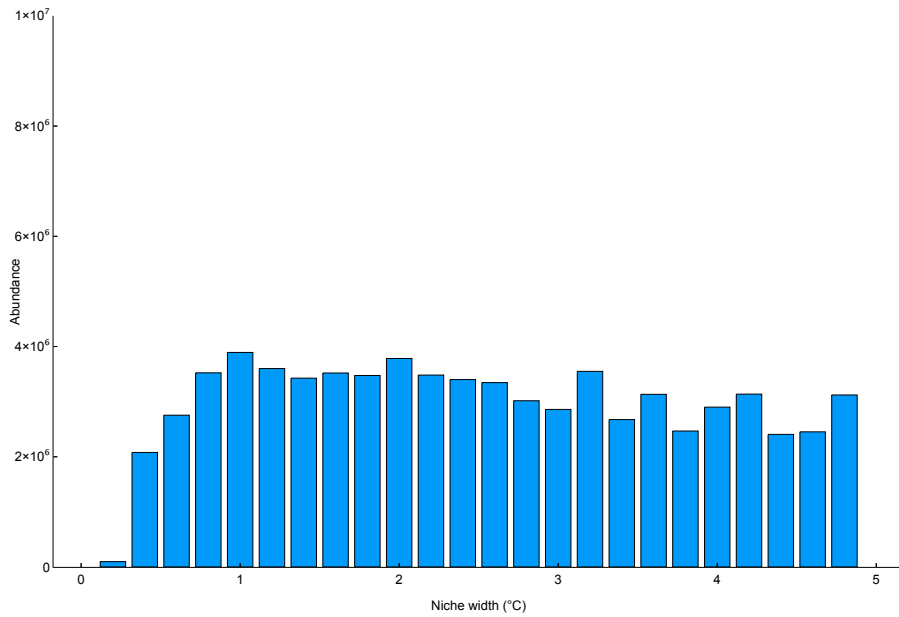


Figure 15: Abundance of species with different niche widths and a temperature preference for 26°C, across 100km² *patch* ecosystem with 100 species and a homogeneous climate of 26°C.

Finally, we ensured that a full complement of species could be supported by the model, especially over large areas and numbers of species (Figure 16). The smaller patches tended to have more stochastic extinctions of species than regions or continents

as we would expect for the ratio of land area (approximately total abundance) to species in the model ($1 \text{ km}^2/\text{species}$, $10 \text{ km}^2/\text{species}$, $20 \text{ km}^2/\text{species}$). At the continent level, the model can comfortably support 10,000 species.

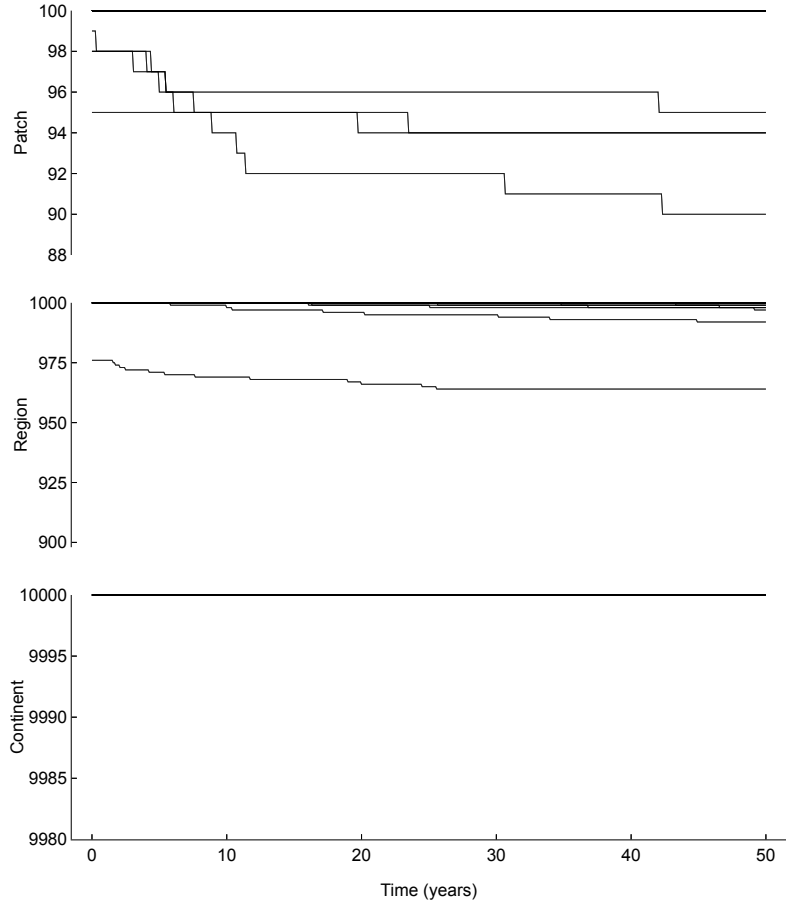


Figure 16: Species richness across 50 repeats of patch, region and continent ecosystems respectively.

5.2 Simulation Experiments

For each of the different habitat types and environmental change scenarios, we ran 100 repeats of the simulation, an example of which can be seen in Figures 17 and 18. For the following plots we will summarise the repeats into composite plots, comparing each diversity measure, scenario and habitat type. However, looking at the runs of the ecosystems over time without any introduced environmental change, it becomes immediately apparent that it is difficult to classify an ecosystem as “stable”, despite adequate “burn ins” and parameter choices. For the span of different biodiversity measures we chose, there is no consensus of whether the ecosystem is stable, in decline or increasing in biodiversity. According to most abundance based measures, such as Sørenson, arithmetic and geometric mean abundance, there is little change over time,

although in some repeats there are marked increases in mean abundance. Species richness also remains relatively stable, despite some stochastic extinctions. On the other hand, more evenness-based measures such as Simpson index and Shannon entropy, as well as normalised and raw alpha and gamma, suggest that there are changes in the relative abundance of some species over and above these extinctions. Therefore, for the remaining plots (Figures 19 - 42) we examined each scenario minus the values of the “neutral scenario”, in which no change was imposed. Although there is a great deal of change within some runs of the neutral scenarios, there is surprisingly little variability between different realisations of the neutral scenario starting with the same population. In the following sections, we will begin with a descriptive overview of each scenario and ecosystem type, before analysing the results in aggregate.

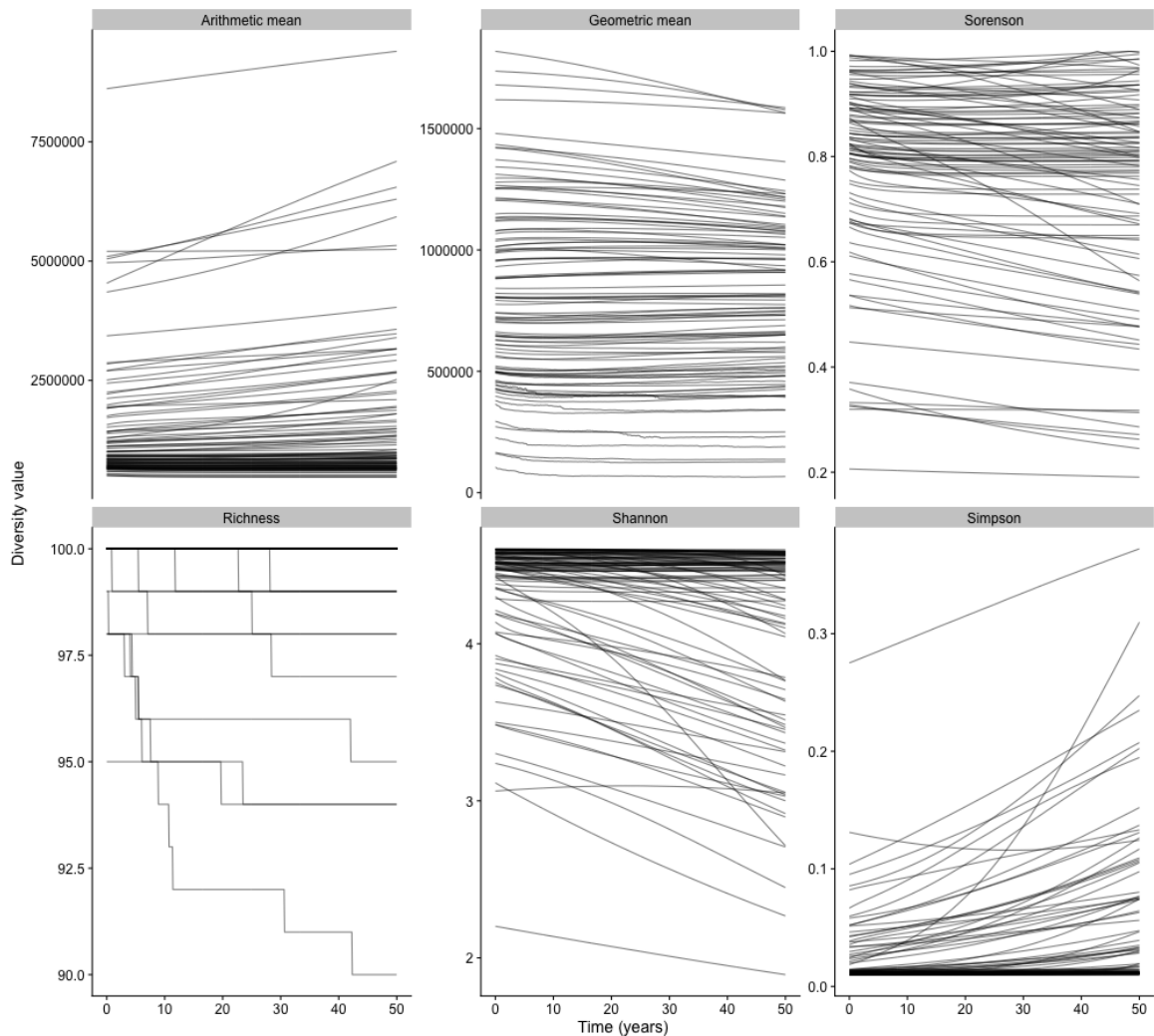


Figure 17: Temporal trends in traditional biodiversity metrics over time across 100km^2 replicate *patch* ecosystems with 100 species and a homogeneous climate of 25°C . The neutral, no change scenario, with each line representing one of 100 replicates per measure.

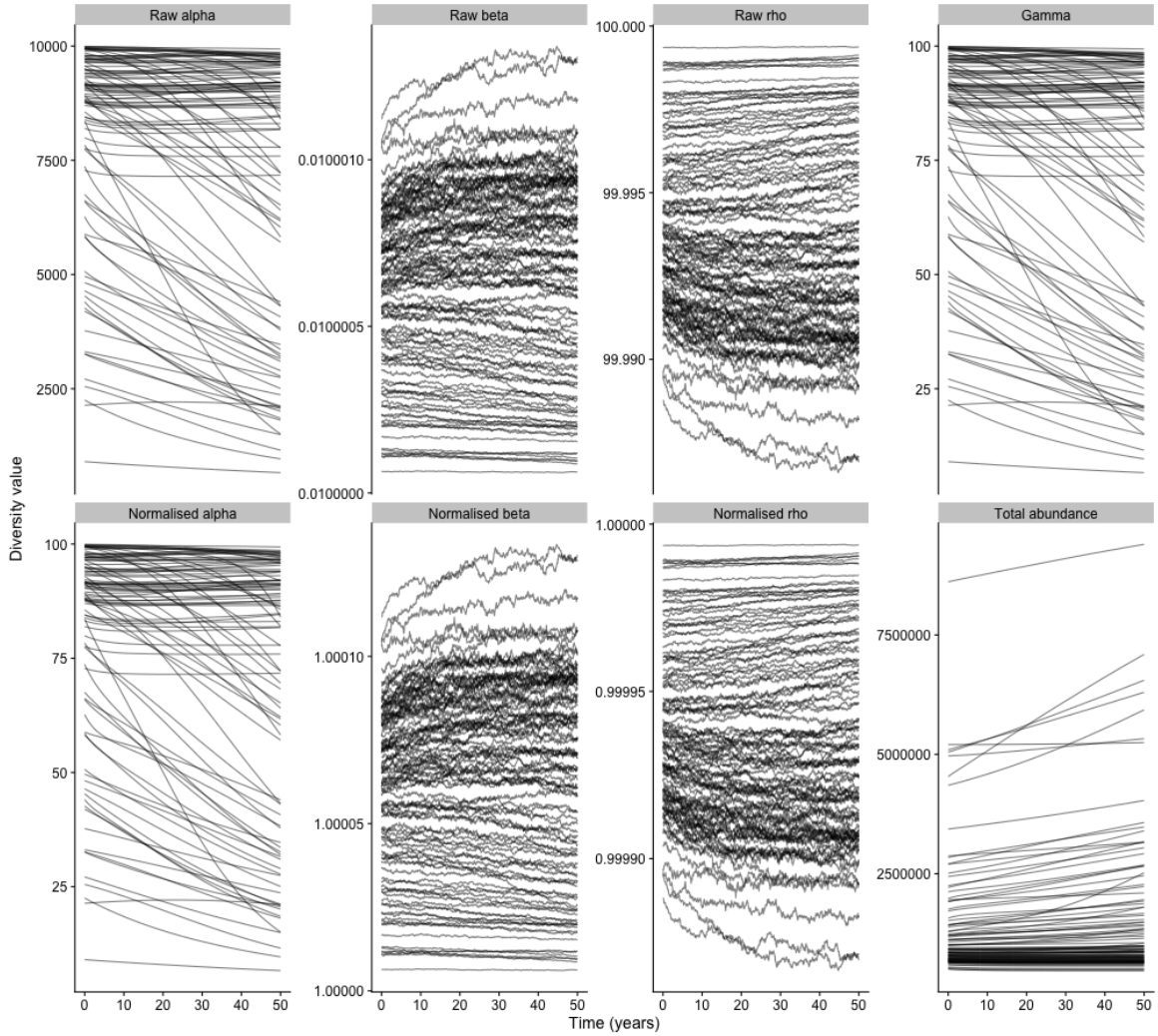


Figure 18: Temporal trends in the diversity framework metrics ($q = 1$) over time across 100km^2 replicate *patch* ecosystems with 100 species and a homogeneous climate of 25°C . The neutral, no change scenario, with each line representing one of 100 replicates per measure.

5.2.1 Patches and Islands

Comparing the ‘island’ (Figures 20, 22) and ‘patch’ (Figures 19, 21) ecosystems with each set of biodiversity measures, the closed borders of the island system were on the whole similar to the open patches, although responses of the biodiversity measures showed slightly more strongly in some cases, e.g. the scenarios of habitat loss, where island habitats promote stronger declines in measures such as Sørenson, richness and Shannon entropy. Most of the traditional measures in Figures 19 and 20 show inconsistent responses across the repeats. However, geometric mean abundance shows the strongest and most consistent trends in all scenarios, especially the temperature increase scenarios. Conversely, species richness shows little change across all scenarios, except for random habitat loss. Alpha and gamma diversity at $q = 1$ have a similarly

broad span of positive and negative responses to most scenarios (Figures 21 and 22). The scenarios of habitat loss produce the most consistent changes in diversity metric for those concerned with beta or between subcommunity, diversity. In particular, local patches become less redundant (raw rho) and less representative of the ecosystem as a whole (normalised rho), as they become more distinct (raw beta).

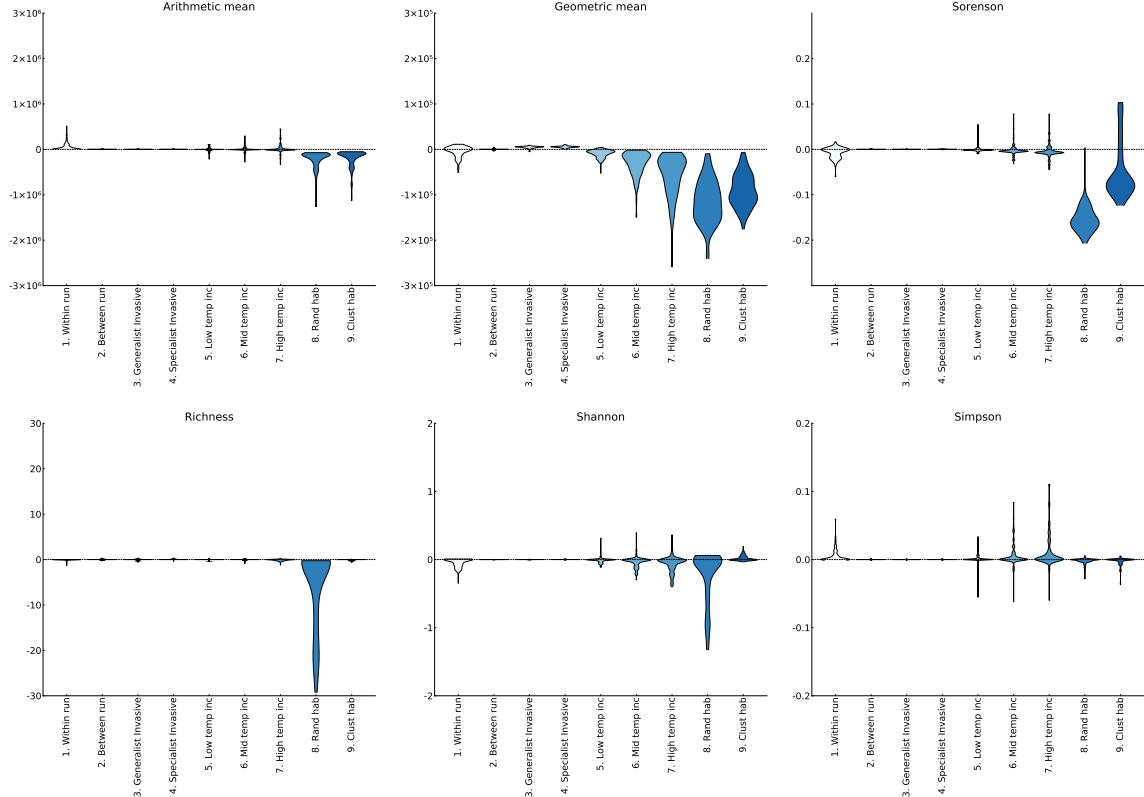


Figure 19: Decadal rate of change in traditional biodiversity measures compared to neutral scenario across 100km^2 replicate *patch* ecosystems with 100 species and a homogeneous climate of 25°C . The x axis indicates the type of ecosystem change applied (see Table 3) and the width of each bar represents the concentration of diversity values.

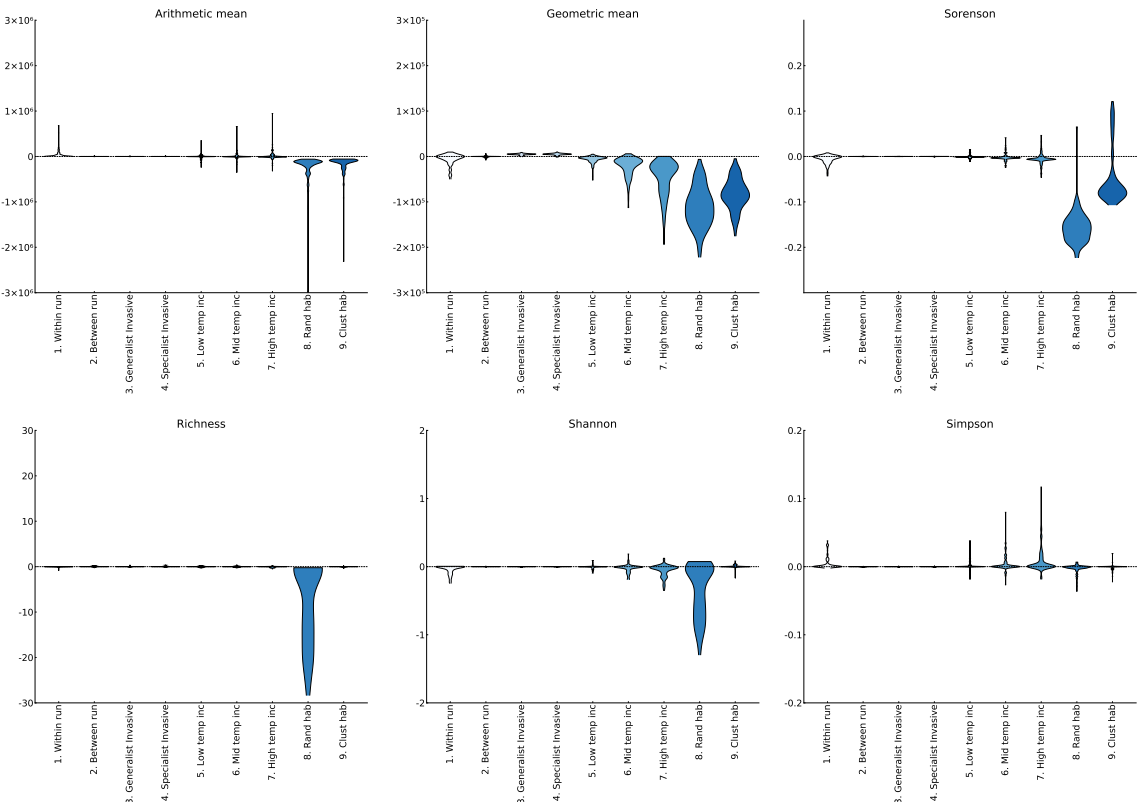


Figure 20: Decadal rate of change in traditional biodiversity measures compared to neutral scenario across 100km² replicate *island* ecosystems with 100 species and a homogeneous climate of 25°C. The x axis indicates the type of ecosystem change applied (see Table 3) and the width of each bar represents the concentration of diversity values.

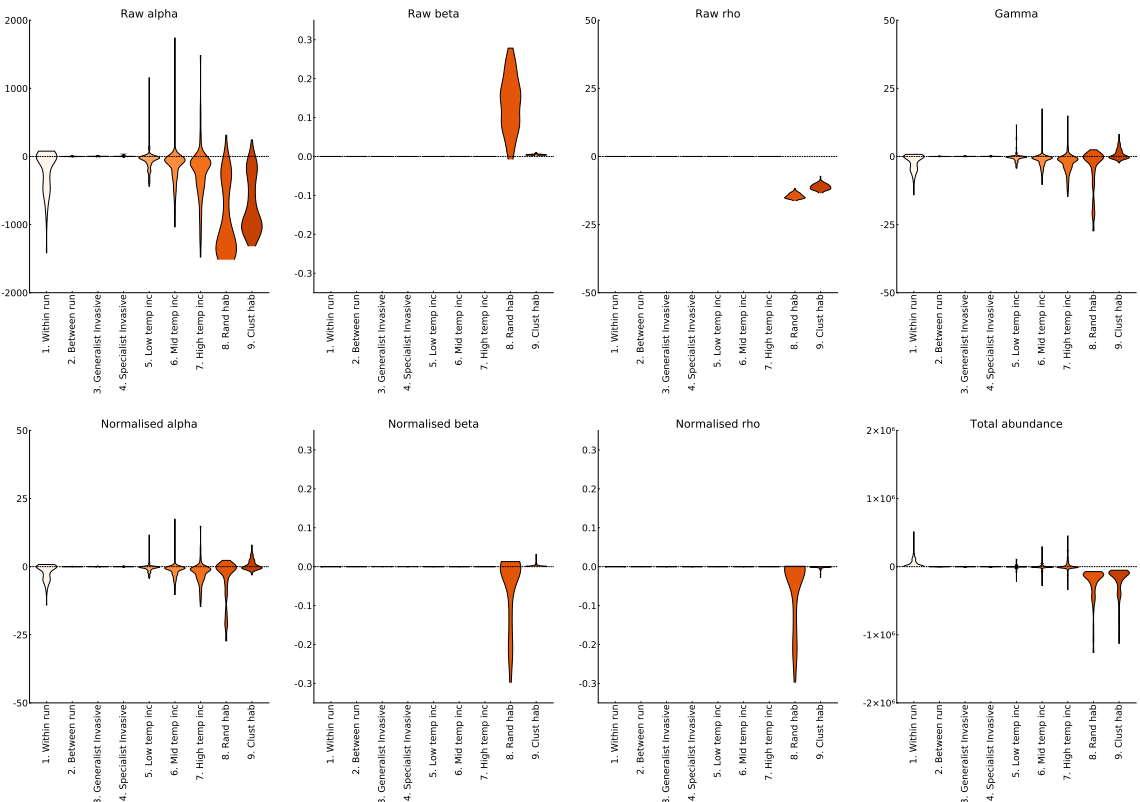


Figure 21: Decadal rate of change in framework biodiversity measures compared to neutral scenario across 100km^2 replicate *patch* ecosystems with 100 species and a homogeneous climate of 25°C . The x axis indicates the type of ecosystem change applied (see Table 3) and the width of each bar represents the concentration of diversity values.

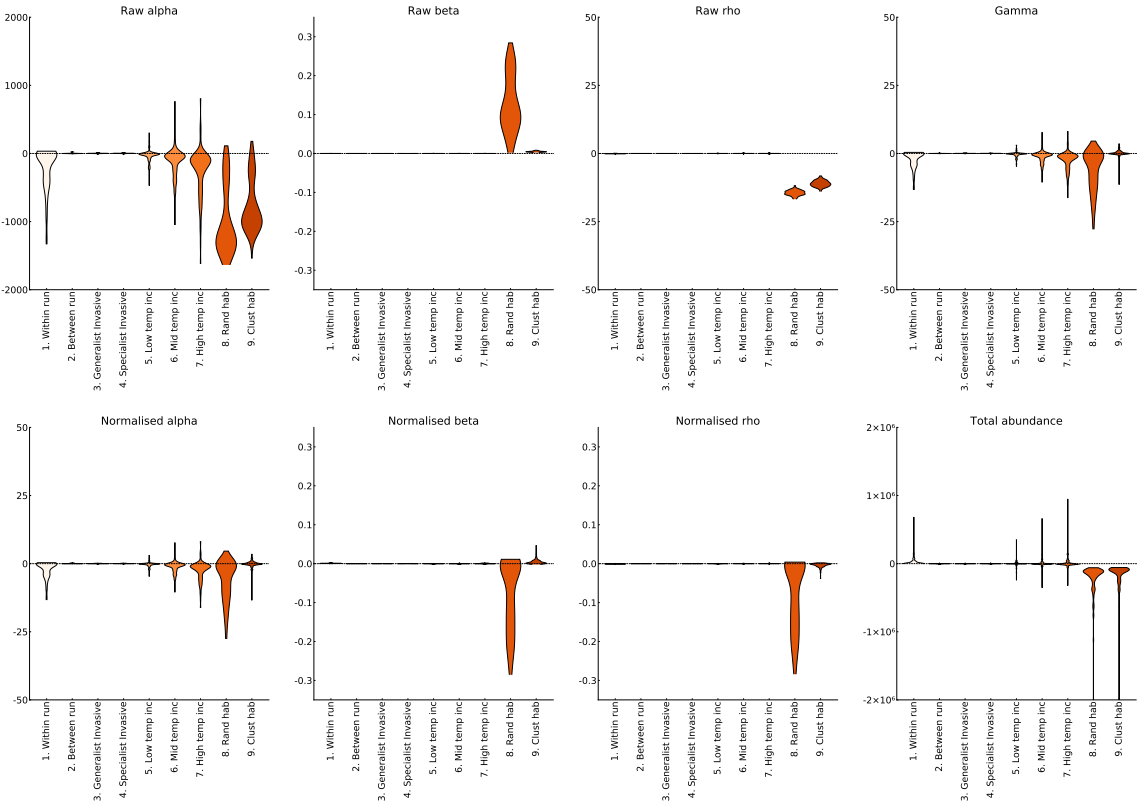


Figure 22: Decadal rate of change in framework biodiversity measures compared to neutral scenario across 100km^2 replicate *island* ecosystems with 100 species and a homogeneous climate of 25°C . The x axis indicates the type of ecosystem change applied (see Table 3) and the width of each bar represents the concentration of diversity values.

5.2.2 Regions

For the regional-scale ecosystems in the experiments, we see changes in the strength of signal across different habitat types and metrics (Figures 23, 24, 25 and 26). These changes in biodiversity are generally stronger in the habitat with the temperature gradient than with the homogenous habitat, with the exception of species richness, where the signal diminishes almost entirely. There are also more consistently unidirectional responses in the gradient habitat, for example the strong positive and negative slopes in the Simpson and Shannon measures. This consistency and strength in gradient habitats compared to even also generally applies to the diversity framework, particularly regarding the temperature increase scenarios.

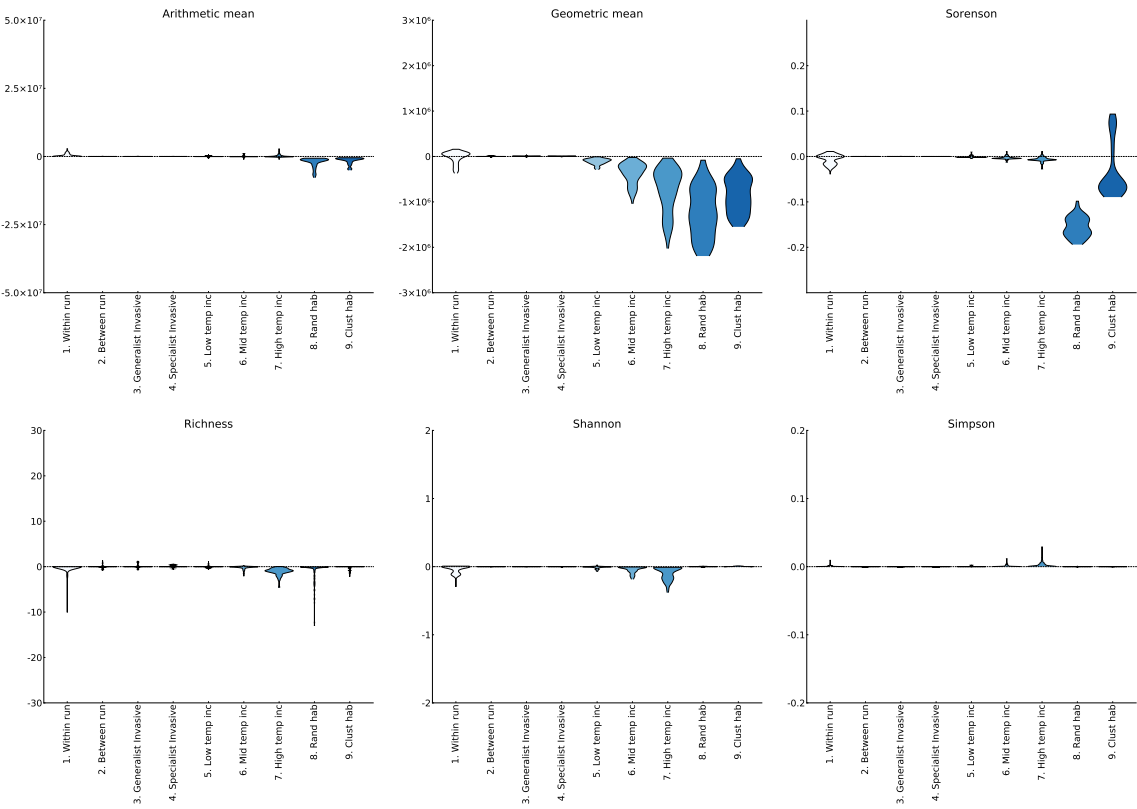


Figure 23: Decadal rate of change in traditional biodiversity measures compared to neutral scenario across 10,000km² replicate *region* ecosystems with 1,000 species and an even climate of 25°C. The x axis indicates the type of ecosystem change applied (see Table 3) and the width of each bar represents the concentration of diversity values.

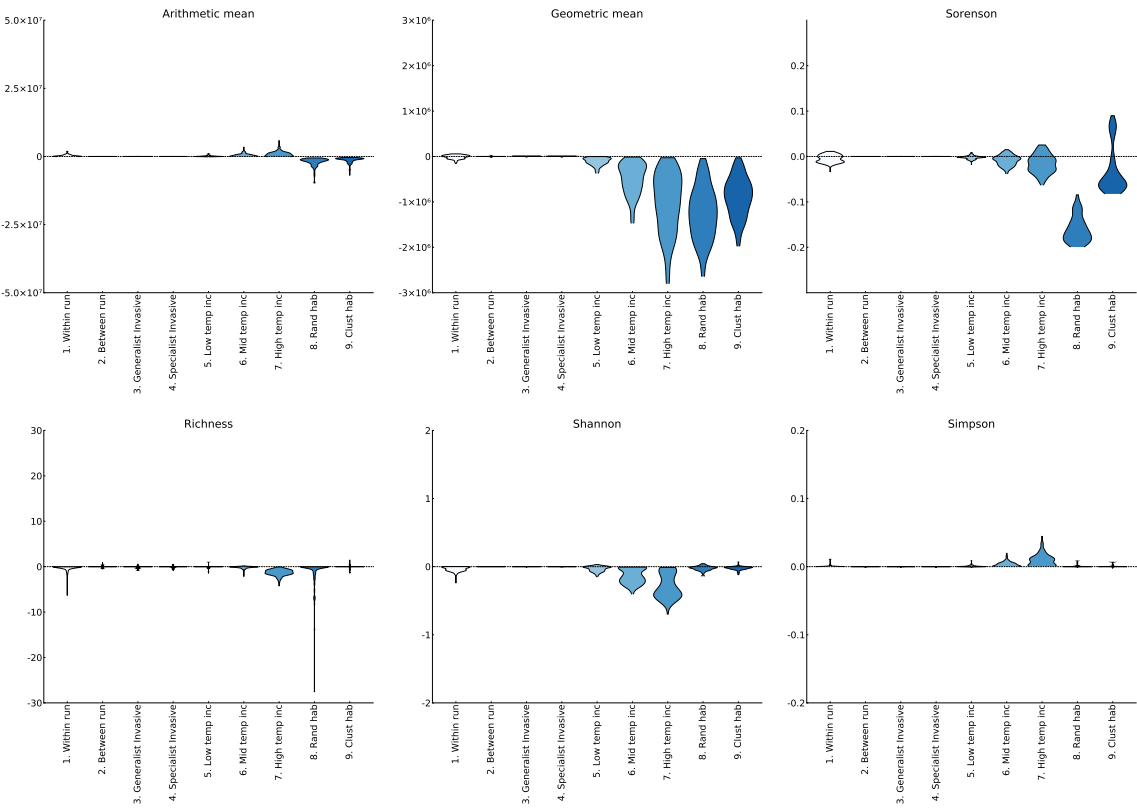


Figure 24: Decadal rate of change in traditional biodiversity measures compared to neutral scenario across 10,000km² replicate *region* ecosystems with 1,000 species and a climate with a linear gradient ranging from 20°C to 30°C. The x axis indicates the type of ecosystem change applied (see Table 3) and the width of each bar represents the concentration of diversity values.

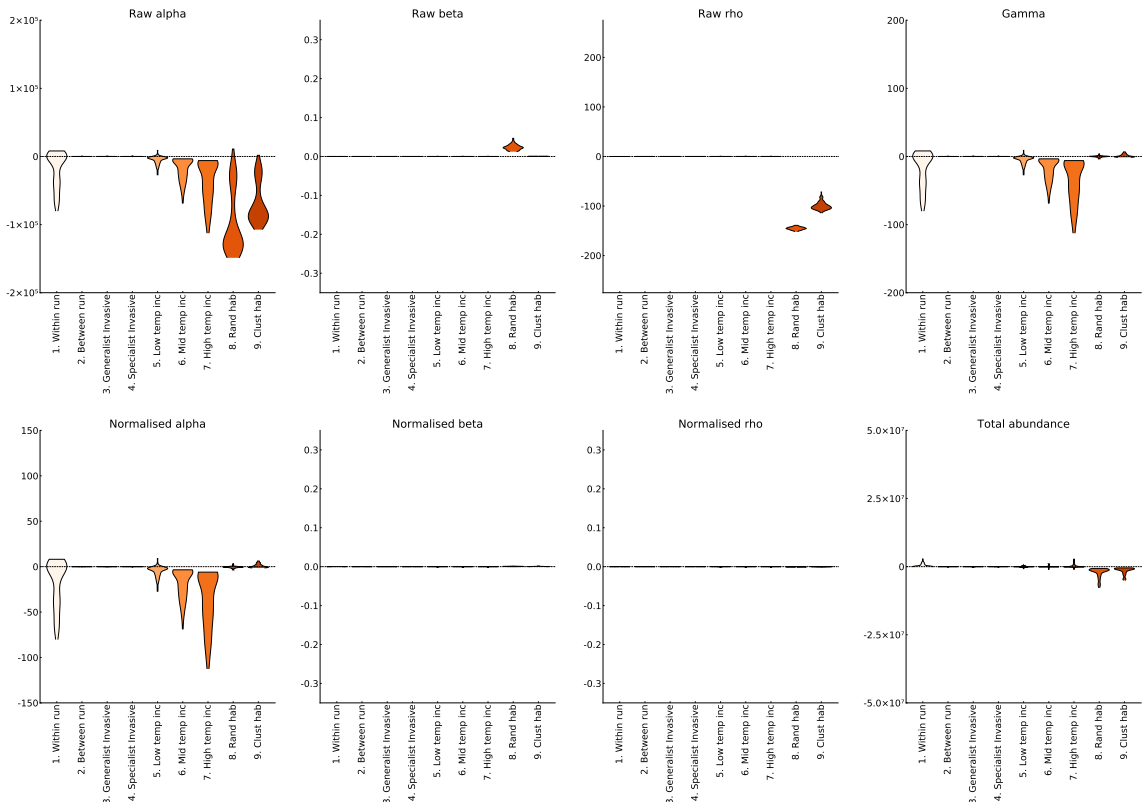


Figure 25: Decadal rate of change in framework biodiversity measures compared to neutral scenario across $10,000\text{km}^2$ replicate *region* ecosystems with 1,000 species and an even climate of 25°C . The x axis indicates the type of ecosystem change applied (see Table 3) and the width of each bar represents the concentration of diversity values.

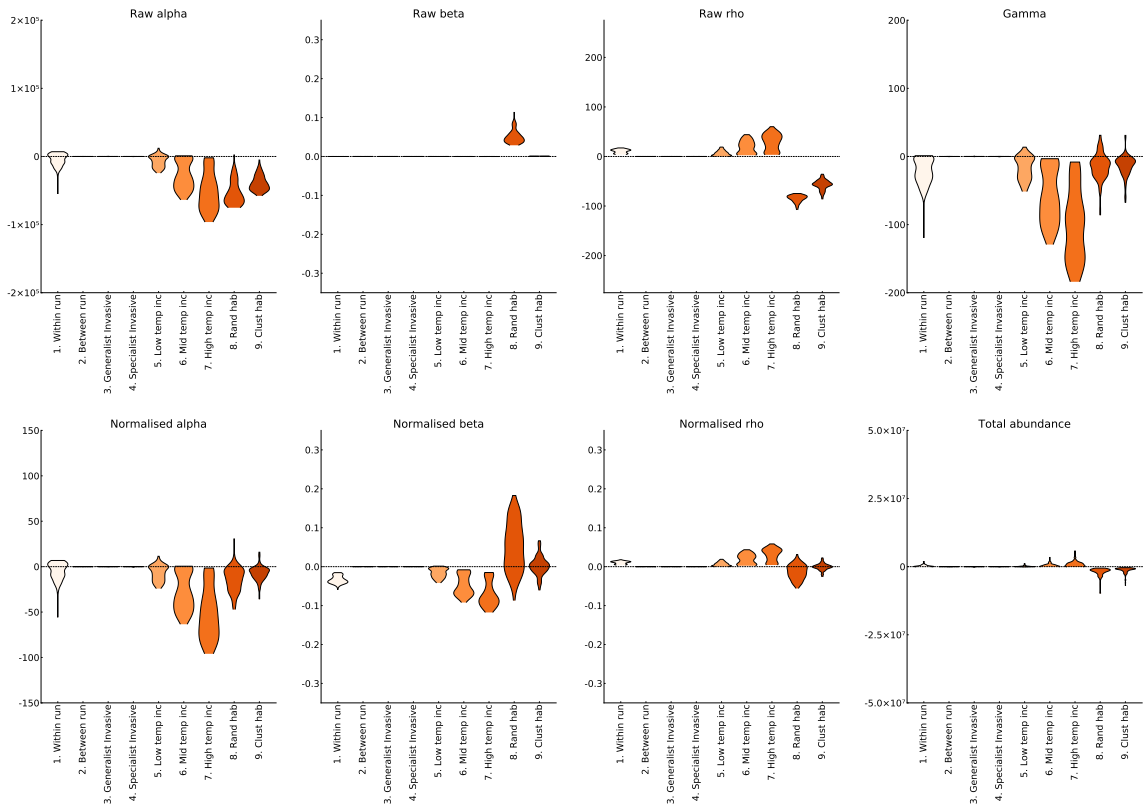


Figure 26: Decadal rate of change in framework biodiversity measures compared to neutral scenario across 10,000km² replicate *region* ecosystems with 1,000 species and a climate with a linear gradient ranging from 20°C to 30°C. The x axis indicates the type of ecosystem change applied (see Table 3) and the width of each bar represents the concentration of diversity values.

5.2.3 Continents

On a continental scale, the temperature had a gradient that peaked in the middle and became cooler at the corresponding ‘poles’. In this system, there is even more consistency in responses of biodiversity metrics (Figures 27 and 28). This is especially apparent in the different temperature increase scenarios, in which the system becomes progressively less abundant (arithmetic mean and geometric mean) and less even (Simpson and Shannon). In contrast, there is very little signal from species richness and Sørenson, although there is a 3-6% decrease in species over the course of the high temperature increase scenario. On the other hand, the diversity framework metrics show corresponding declines in local diversity and contribution to overall diversity that are not captured in regular abundance measures. There is a decline in the effective number of distinct communities (normalised beta), as grid squares become more redundant (raw rho) and less representative of the ecosystem as a whole (normalised rho). Although the traditional measures capture the change in abundance of the habitat loss scenarios, they do not reflect much change in community composition. However, the diversity framework shows a strong increase in distinctiveness of communities (raw

beta) as they become less representative of the ecosystem. This effect is stronger under the random habitat loss scenario compared to the clustered loss.

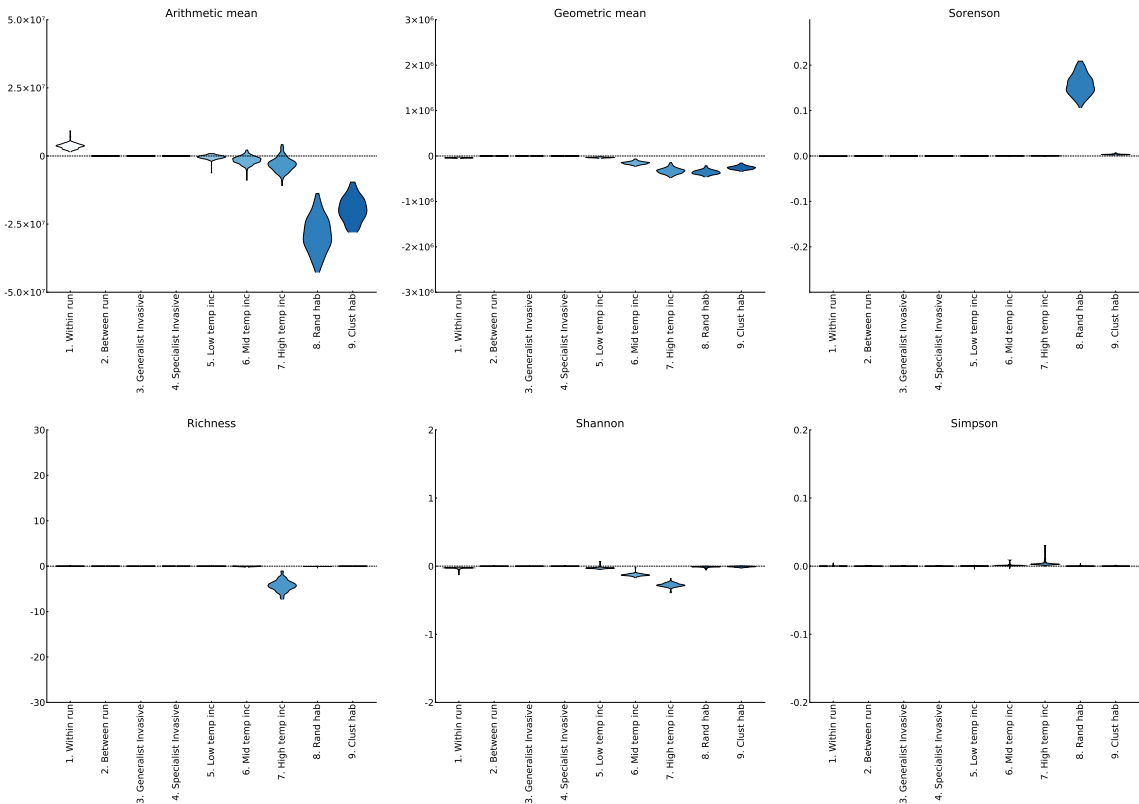


Figure 27: Decadal rate of change in traditional biodiversity measures compared to neutral scenario across 200,000km² replicate *continent* ecosystems with 10,000 species. The x axis indicates the type of ecosystem change applied (see Table 3) and the width of each bar represents the concentration of diversity values.

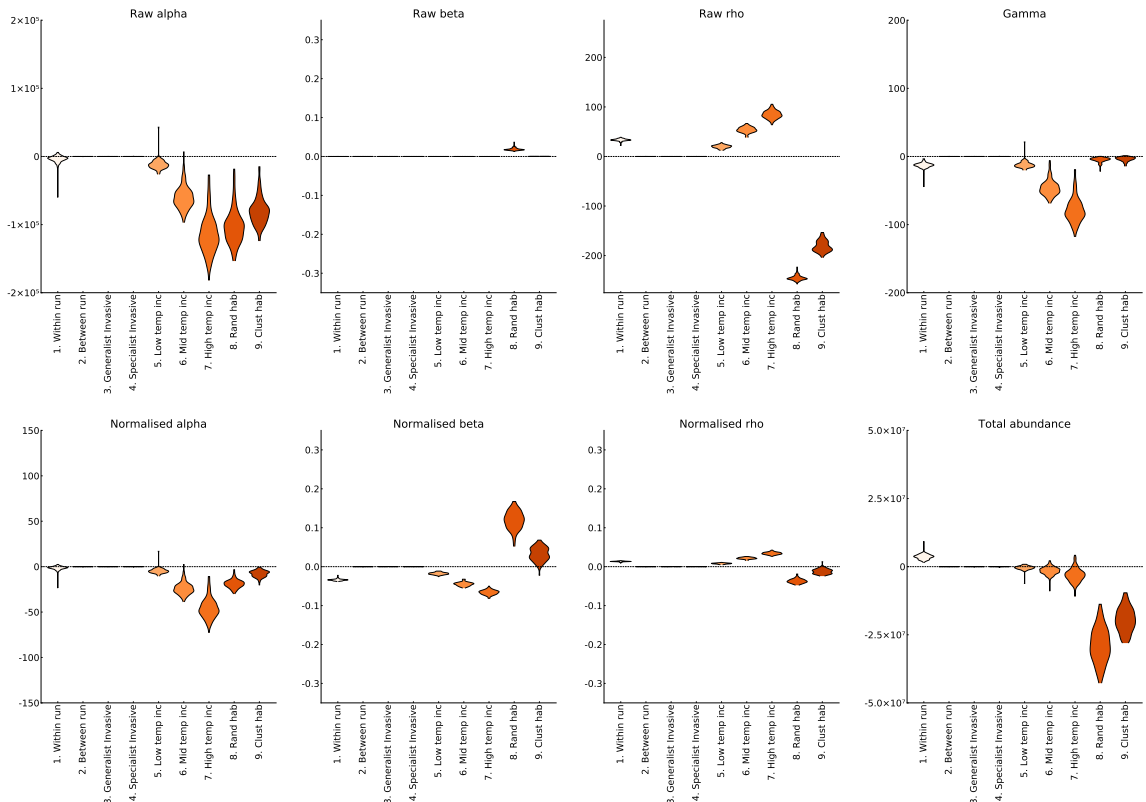


Figure 28: Decadal rate of change in framework biodiversity measures compared to neutral scenario across 200,000km² replicate *continent* ecosystems with 10,000 species. The x axis indicates the type of ecosystem change applied (see Table 3) and the width of each bar represents the concentration of diversity values.

5.2.4 Analysis

In order to understand the ability of the metrics to detect early warnings of biodiversity change, we also calculated the time at which they exceeded ± 2 standard deviations of the neutral scenario. This can be seen in Figure 29 where we have plotted the change in normalised alpha, beta and rho, as well as gamma diversity for the low, medium and high temperature scenarios for the regional simulation. As the temperature change becomes more extreme it is easier for the measures to detect changes earlier. In this case, normalised rho, or average representativeness shows the earliest signal of change, with local communities in the system becoming more representative of the whole ecosystem over time. Comparing across all ecosystem sizes and habitat types (excluding the island, which shows broadly the same responses as the patch) in Figure 30, normalised rho shows the earliest response, closely followed by normalised beta. There is some effect of habitat type and ecosystem size on which scenario is detected first, with the temperature increase scenarios being detected earlier in the gradient and larger systems and the habitat loss being detected earlier in smaller, homogenous habitat systems, where the loss of individual grid squares represent a greater proportion of the whole ecosystem, even though the areas lost were smaller.

Next, we combined the results from all repeats and ecosystem types in Figures 31 and 32 as an overall average of slope of biodiversity measure over time (compared to neutral) with 95% confidence intervals. Overall, geometric mean abundance performs the most consistently across scenarios (without change of sign) from the more traditional metrics (Figure 31). The diversity framework shows comparable decreases in gamma diversity. However, by using this framework, we are also able to deconstruct the relative impacts on community distinctiveness and representativeness that indicate a change in species composition for several scenarios, including climate change and habitat loss. There is little response to either invasive scenario in any of the habitat types or diversity measures.

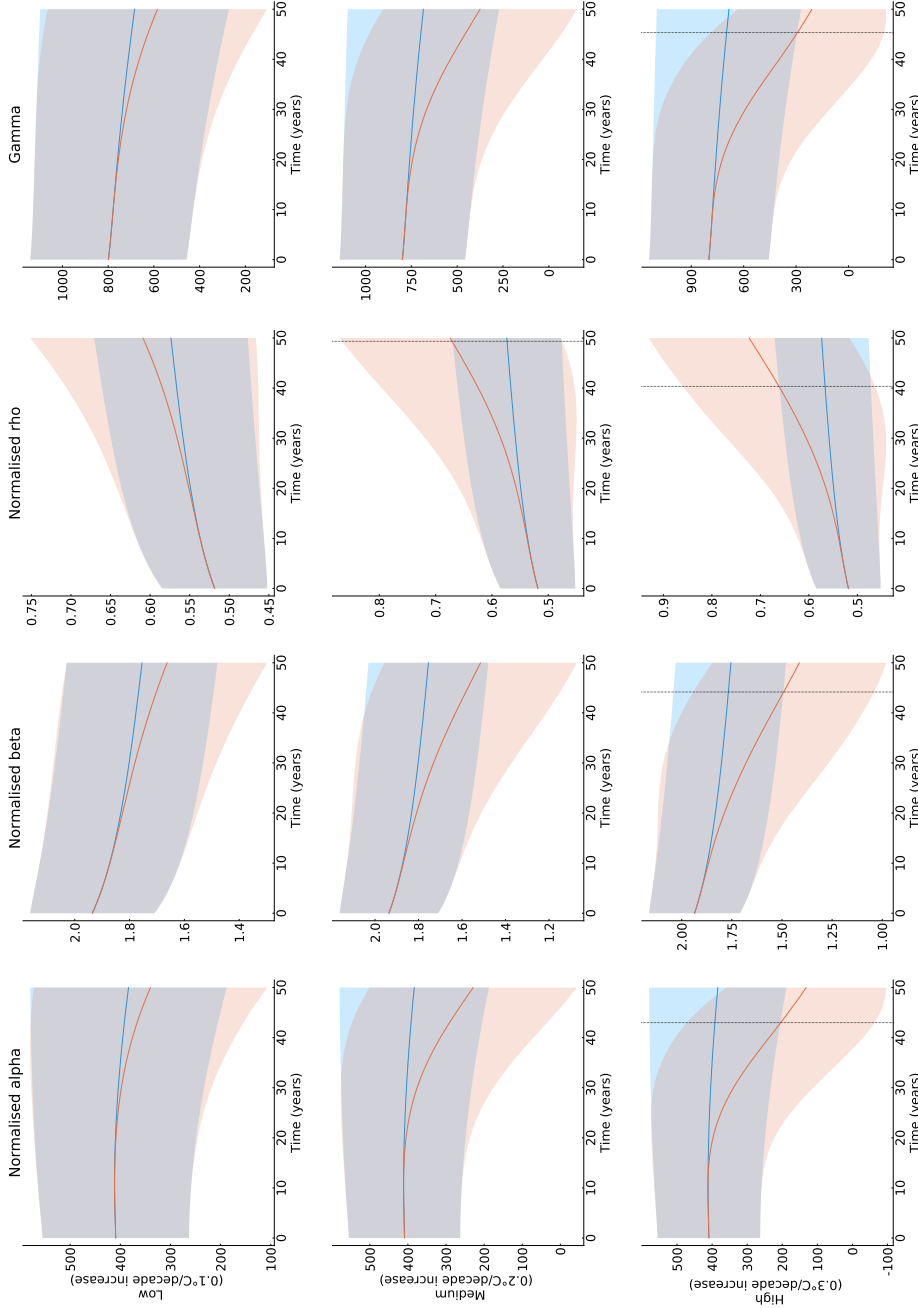


Figure 29: Comparison of the changes in average normalised alpha, normalised beta, normalised rho and gamma diversity over time in low, medium and high temperature ($0.1\text{-}0.3^\circ\text{C}/\text{decade}$) increase scenarios. The simulations were performed on *regional* ecosystems with a $10,000\text{km}^2$ grid with 1,000 species. Blue represents neutral scenarios with no change as a comparison to temperature increase in orange, both with confidence intervals of two standard deviations. The dashed line indicates the time at which change in each indicator extended beyond the stochastic fluctuation from the neutral scenario.

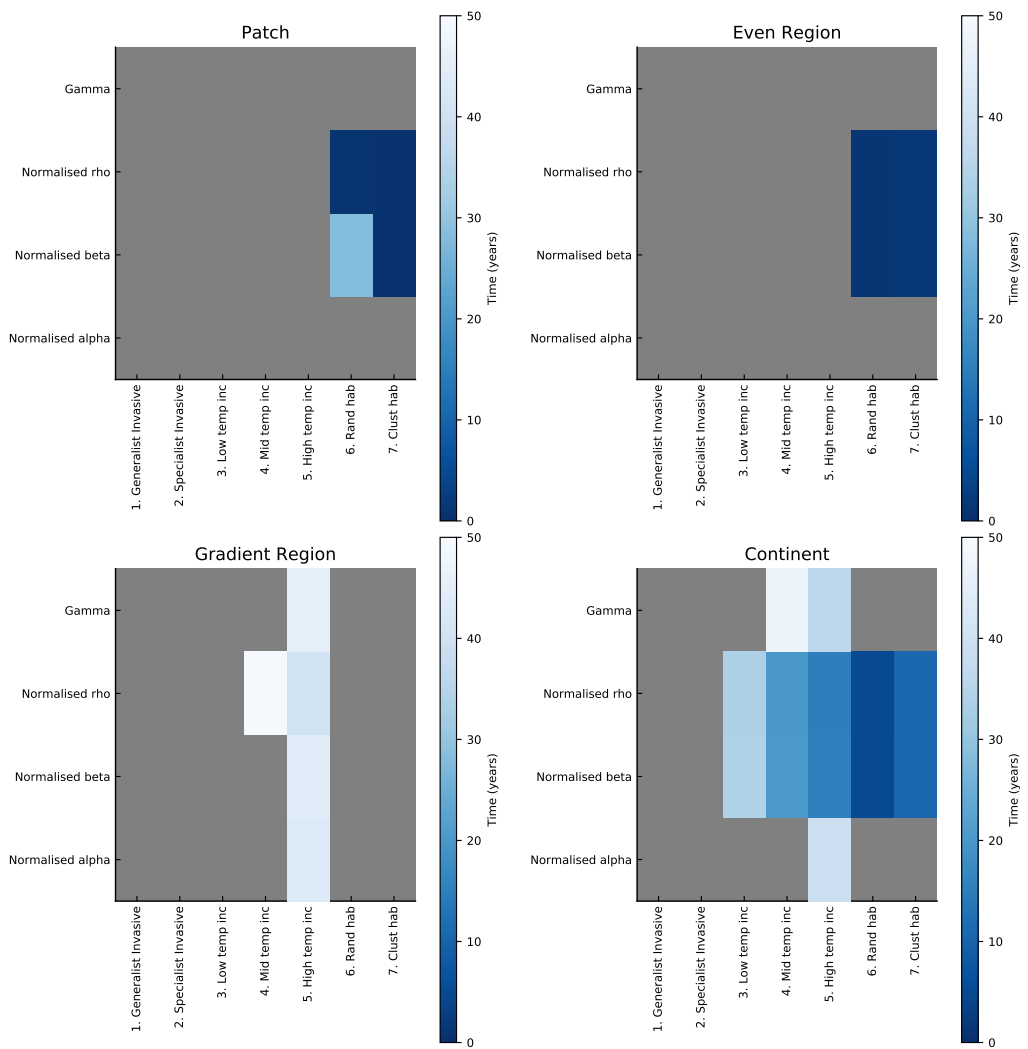


Figure 30: Time taken for average diversity to exceed ± 2 standard deviations of the neutral scenario for patch, region and continental ecosystems. ‘Even Region’ represents regions with a homogenous climate and ‘Gradient Region’ represents regions with a climate gradient. Grey represents no divergence from the neutral scenario in the 50 year time period.

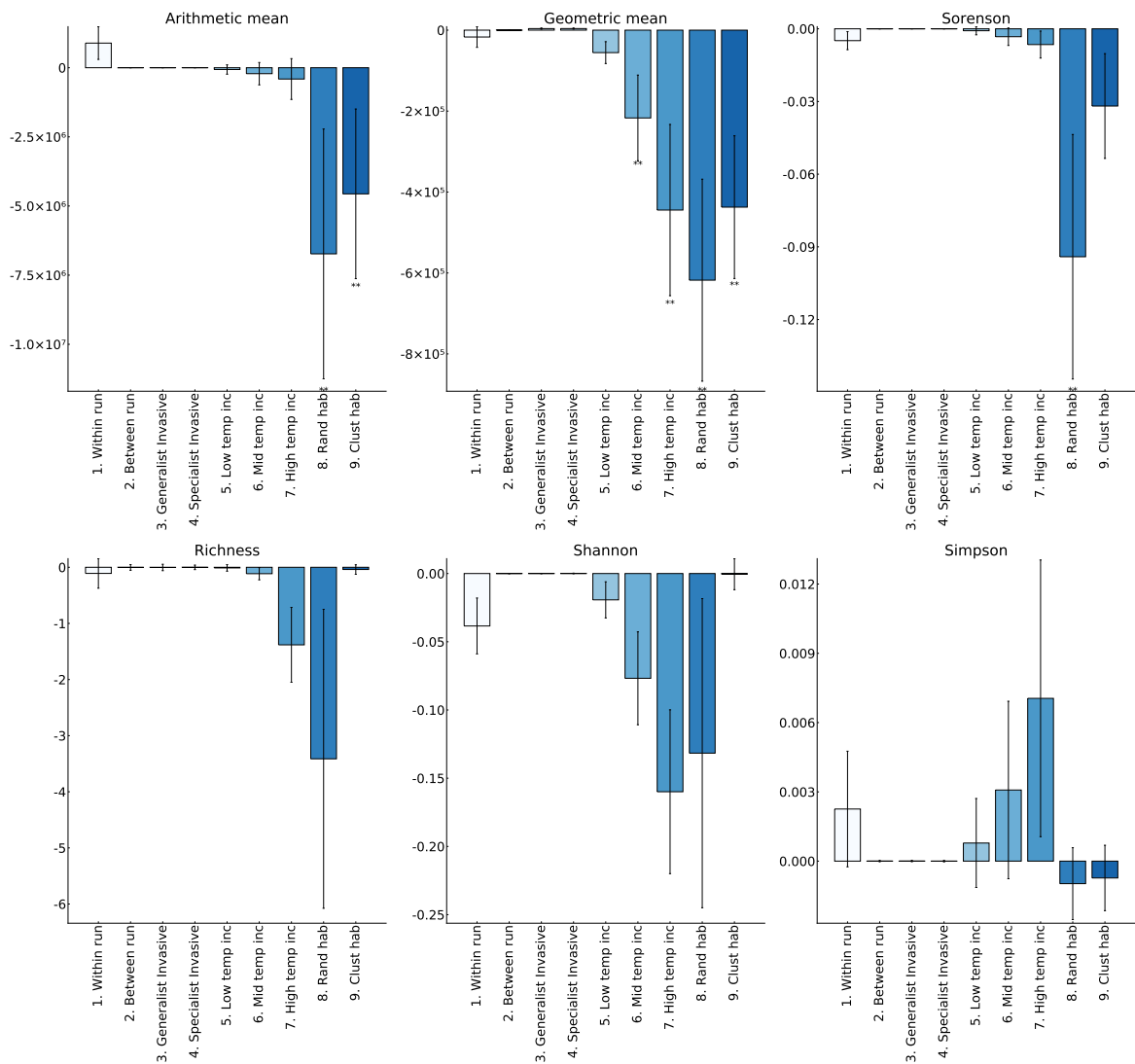


Figure 31: Average decadal rate of change in traditional biodiversity measures compared to neutral scenario across all ecosystems sizes and habitats, with 95% confidence intervals. * indicates consistency in sign over 95% of replicates. ** indicates consistency in sign over 99% of replicates.

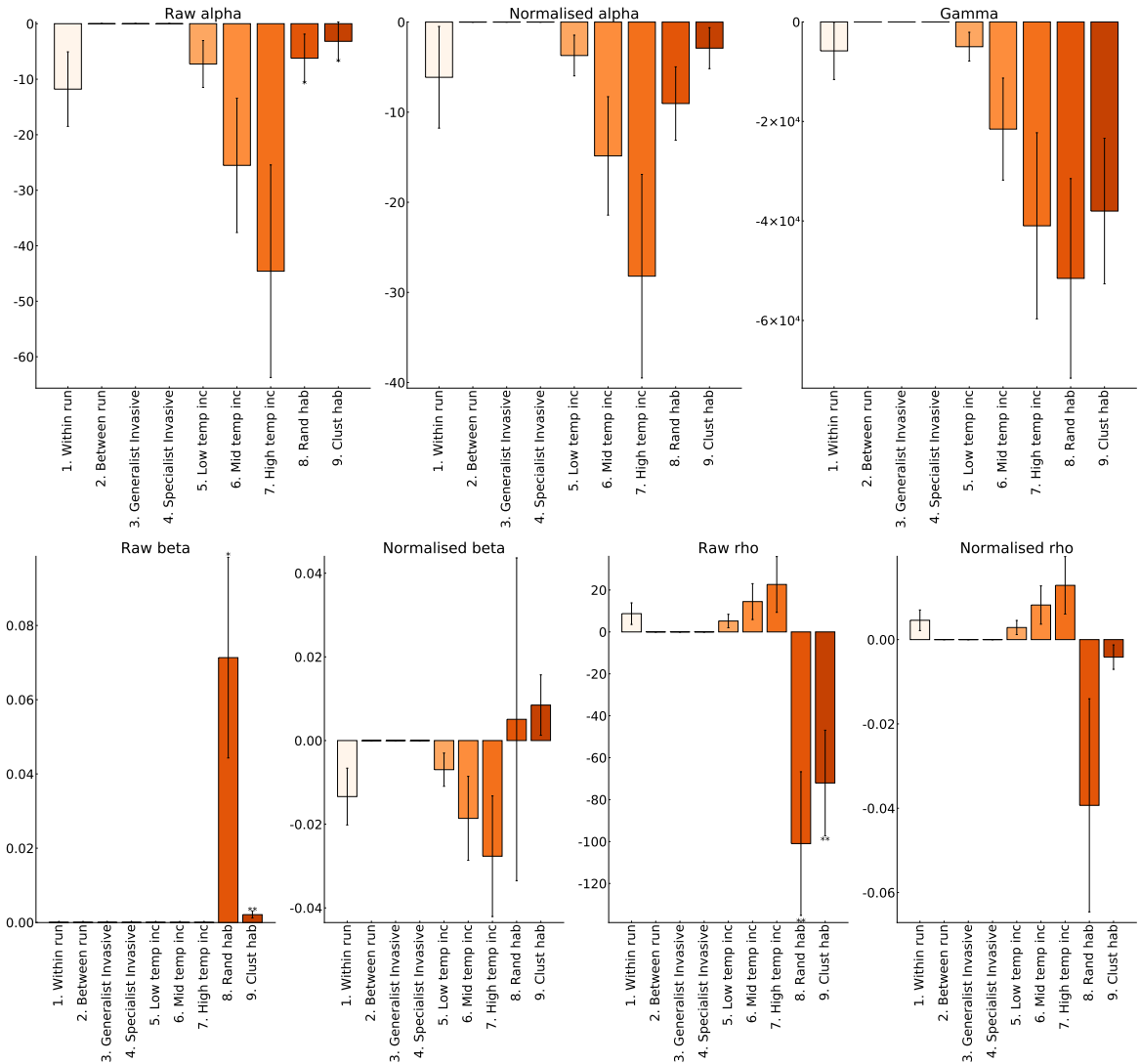


Figure 32: Average decadal rate of change in framework biodiversity measures compared to neutral scenario across all ecosystems sizes and habitats, with 95% confidence intervals. * indicates consistency in sign over 95% of replicates. ** indicates consistency in sign over 99% of replicates.

5.2.5 Temperature fluctuations

Once a sinusoidal “seasonal” background fluctuation was added to the climates (with a magnitude of 5°C, Figure 7), all trends in the diversity measures are lost and all measures have inconsistent directionality between replicates against the noisier fluctuating neutral signal. However, there was some evidence of consistent decline in species, as well as increases in local diversity and distinctiveness from the diversity framework for the regional ecosystems with a gradient environment. Figures 33 to 42 represent these scenarios for the patch, island and regional systems.

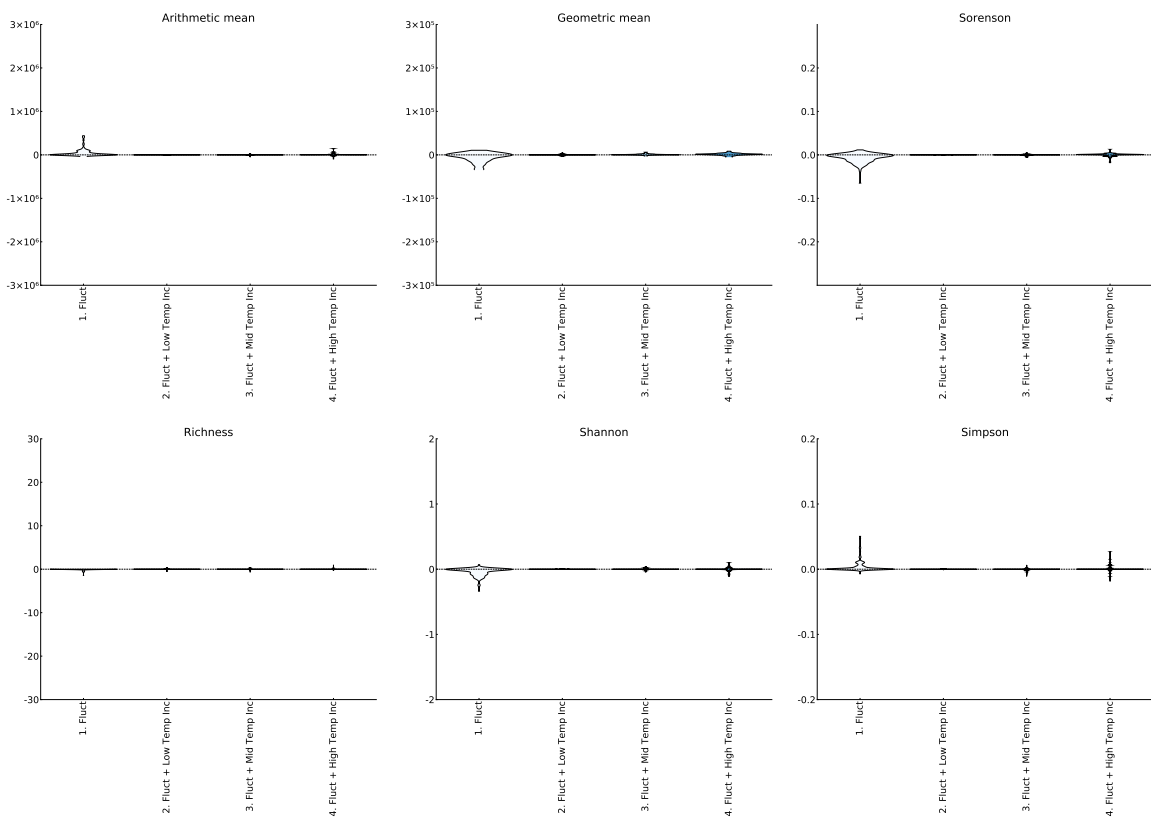


Figure 33: Decadal rate of change in traditional biodiversity measures compared to neutral scenario across 100km² replicate *patch* ecosystems with 100 species and a fluctuating homogeneous climate of 25°C ±5°C. The x axis indicates the type of ecosystem change applied (see Table 3) and the width of each bar represents the concentration of diversity values.

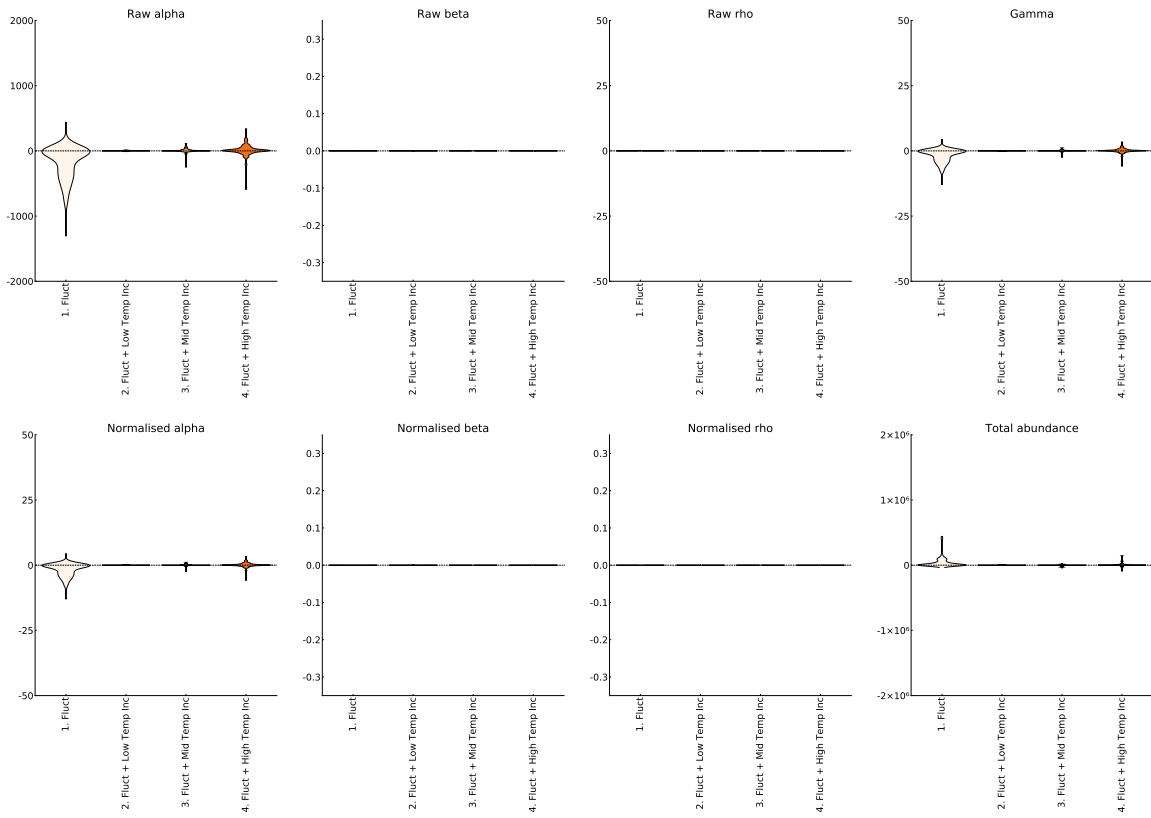


Figure 34: Decadal rate of change in framework biodiversity measures compared to neutral scenario across 100km² replicate *patch* ecosystems with 100 species and a fluctuating homogeneous climate of $25^{\circ}\text{C} \pm 5^{\circ}\text{C}$. The x axis indicates the type of ecosystem change applied (see Table 3) and the width of each bar represents the concentration of diversity values.

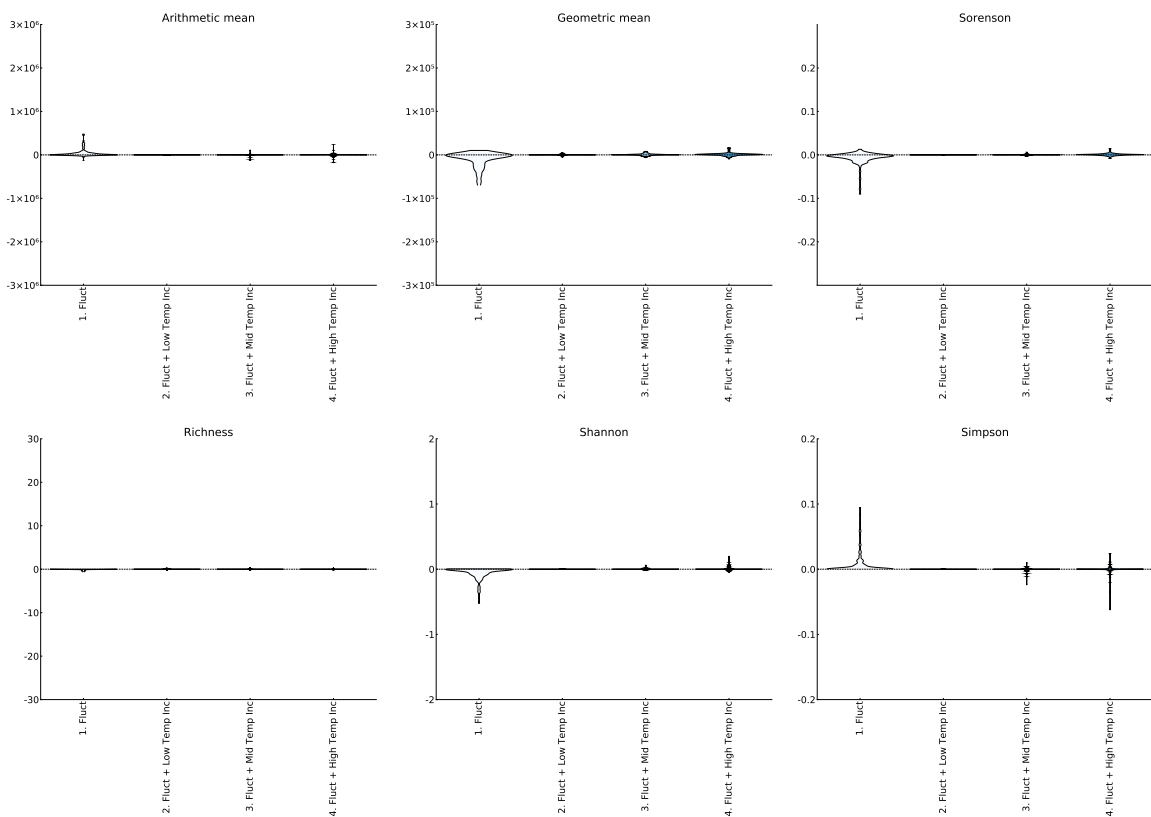


Figure 35: Decadal rate of change in traditional biodiversity measures compared to neutral scenario across 100km² replicate *island* ecosystems with 100 species and a fluctuating homogeneous climate of 25°C ±5°C. The x axis indicates the type of ecosystem change applied (see Table 3) and the width of each bar represents the concentration of diversity values.

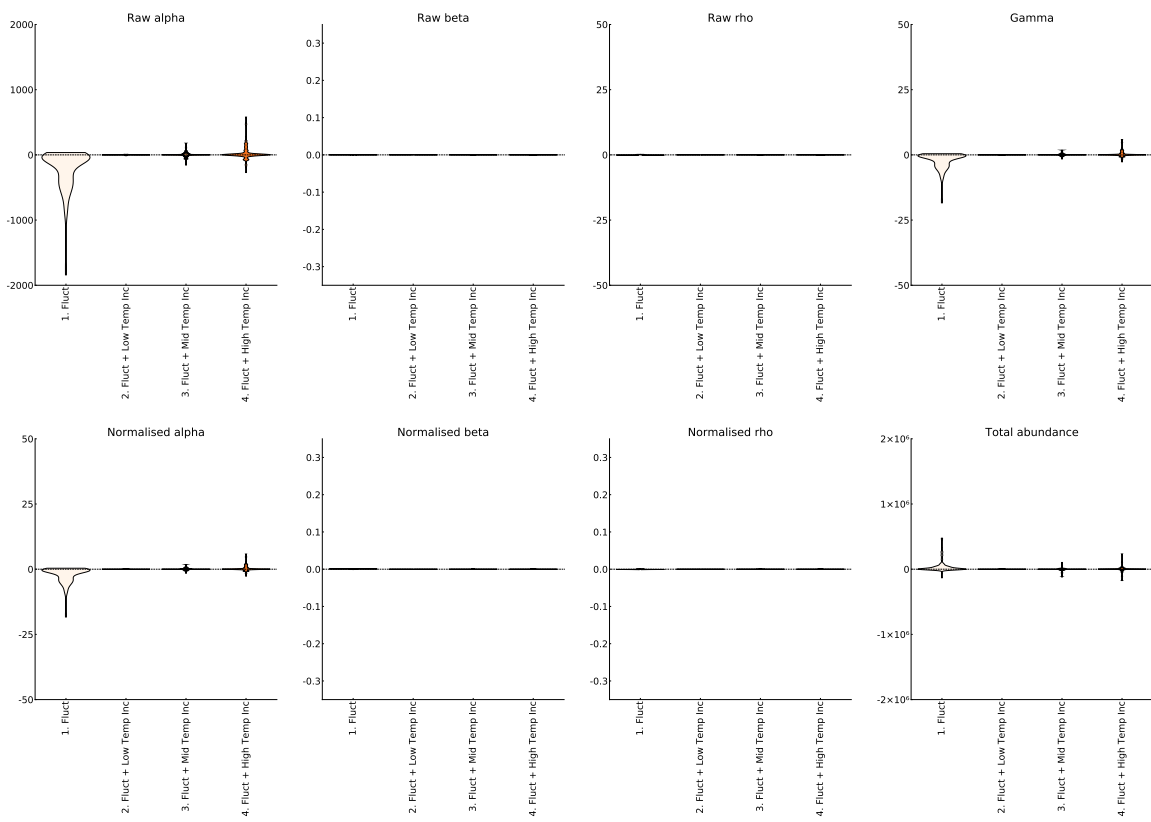


Figure 36: Decadal rate of change in framework biodiversity measures compared to neutral scenario across 100km² replicate *island* ecosystems with 100 species and a fluctuating homogeneous climate of 25°C ±5°C. The x axis indicates the type of ecosystem change applied (see Table 3) and the width of each bar represents the concentration of diversity values.

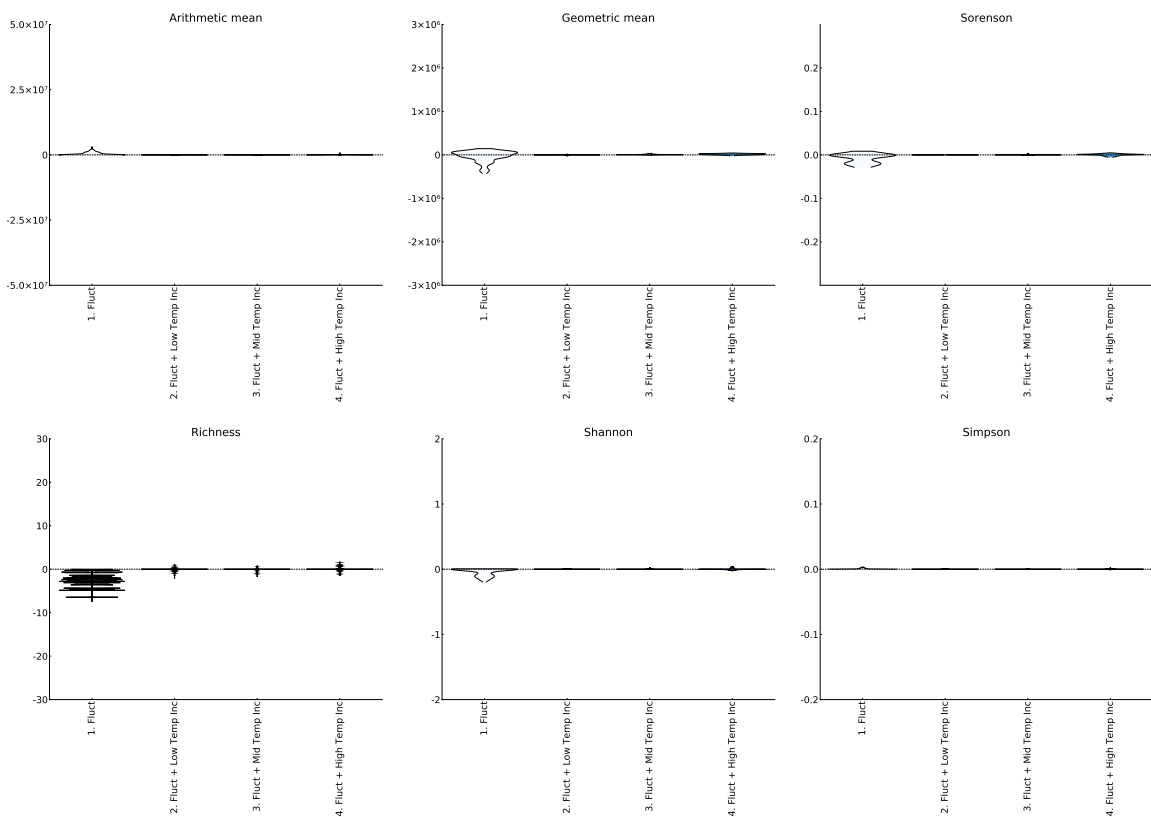


Figure 37: Decadal rate of change in traditional biodiversity measures compared to neutral scenario across 10,000km² replicate *region* ecosystems with 1,000 species and a fluctuating homogeneous climate of 25°C ±5°C. The x axis indicates the type of ecosystem change applied (see Table 3) and the width of each bar represents the concentration of diversity values.

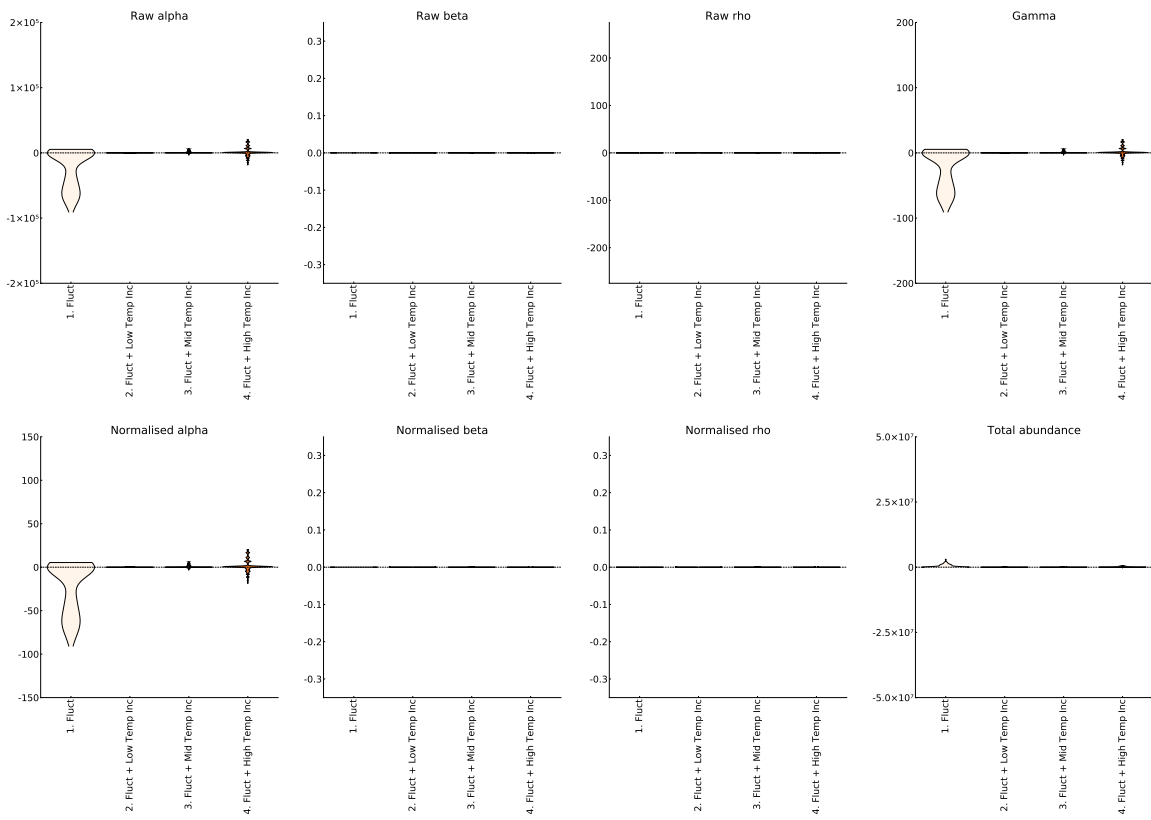


Figure 38: Decadal rate of change in framework biodiversity measures compared to neutral scenario across 100km^2 replicate *island* ecosystems with 1,000 species and a fluctuating homogeneous climate of $25^\circ\text{C} \pm 5^\circ\text{C}$. The x axis indicates the type of ecosystem change applied (see Table 3) and the width of each bar represents the concentration of diversity values.

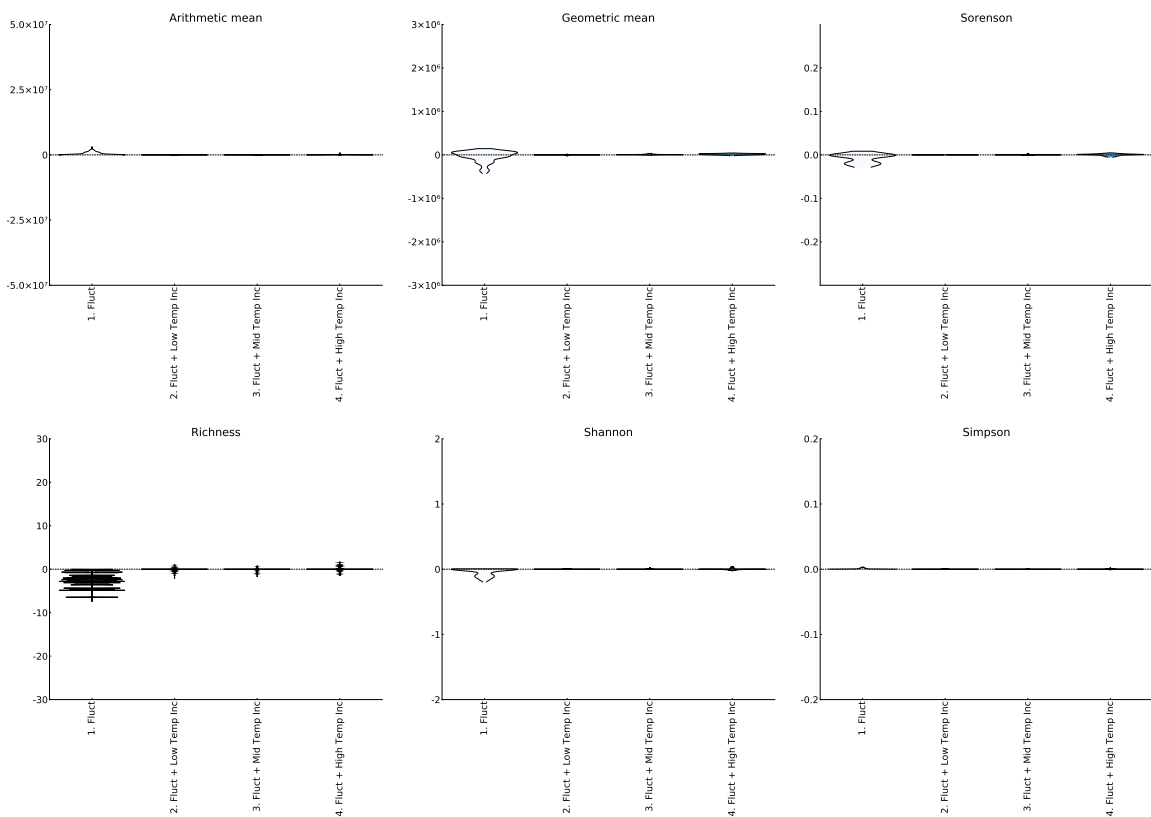


Figure 39: Decadal rate of change in traditional biodiversity measures compared to neutral scenario across 10,000km² replicate *region* ecosystems with 1,000 species and a fluctuating homogeneous climate of 25°C ±5°C. The x axis indicates the type of ecosystem change adopted and the width of each bar represents the concentration of diversity values.

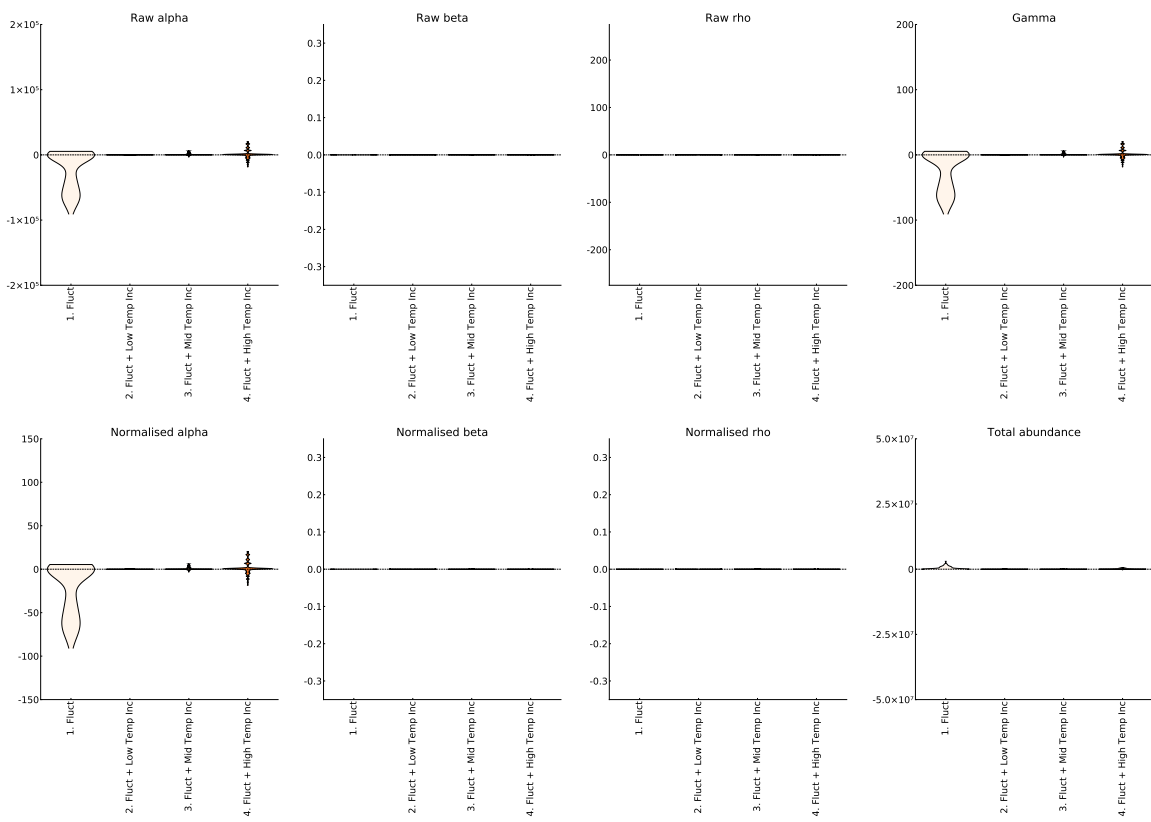


Figure 40: Decadal rate of change in framework biodiversity measures compared to neutral scenario across 100km² replicate *region* ecosystems with 1,000 species and a fluctuating homogeneous climate of 25°C ±5°C. The x axis indicates the type of ecosystem change adopted and the width of each bar represents the concentration of diversity values.

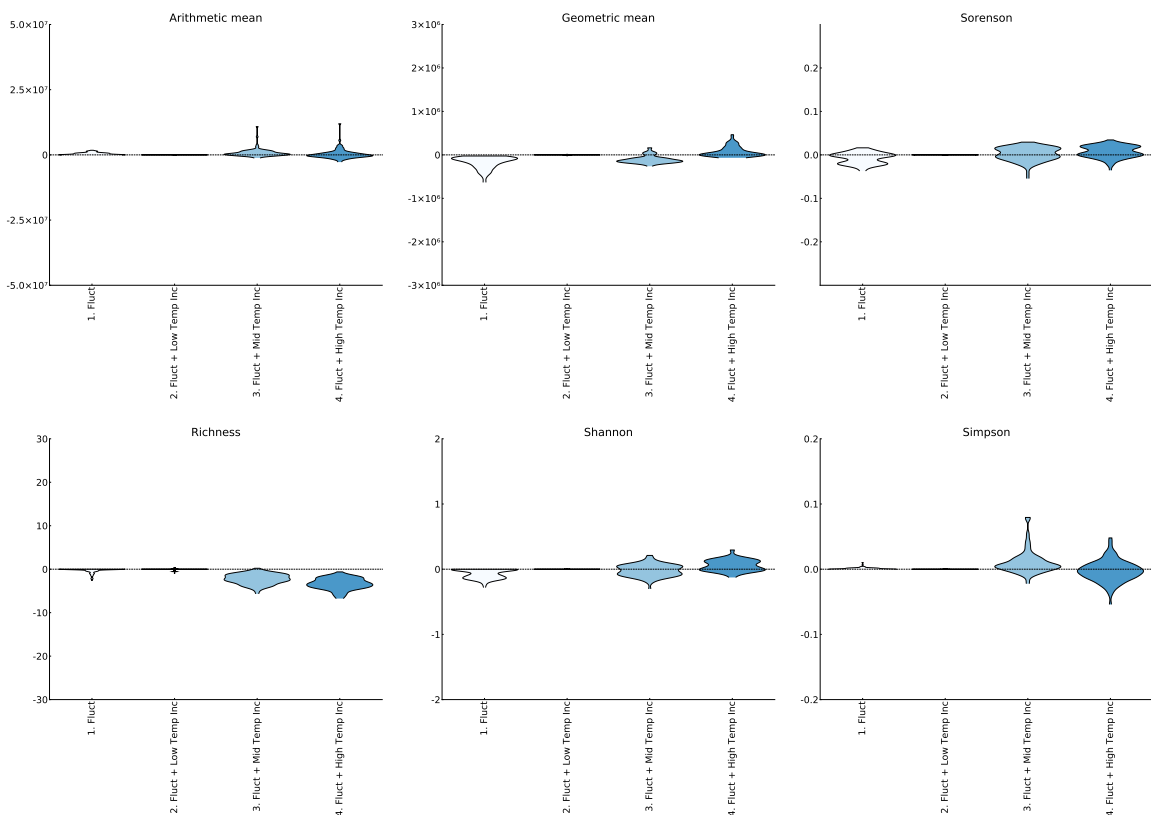


Figure 41: Decadal rate of change in traditional biodiversity measures compared to neutral scenario across 10,000km² replicate *region* ecosystems with 1,000 species and a climate with a linear gradient ranging from 20°C to 30°C, plus a fluctuation of $\pm 5^\circ\text{C}$. The x axis indicates the type of ecosystem change adopted and the width of each bar represents the concentration of diversity values.

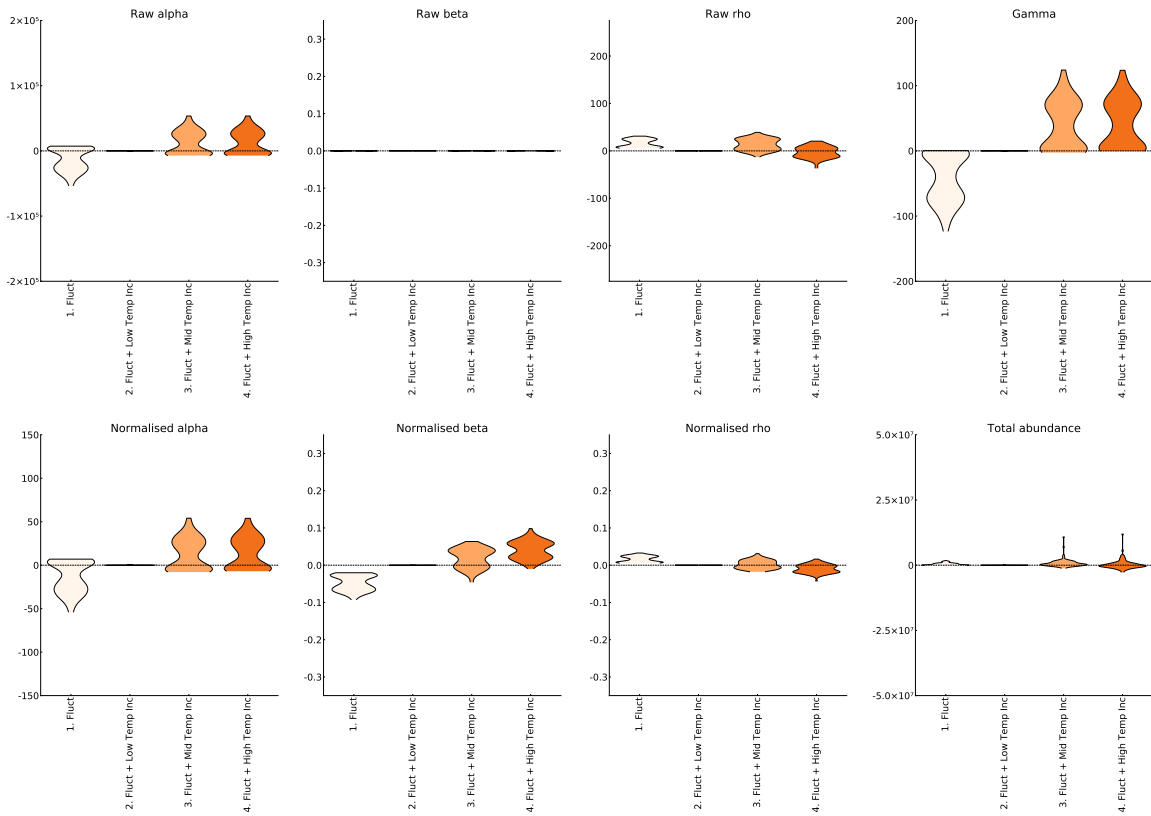


Figure 42: Decadal rate of change in framework biodiversity measures compared to neutral scenario across 100km^2 replicate *region* ecosystems with 1,000 species and a fluctuating homogeneous climate of $25^\circ\text{C} \pm 5^\circ\text{C}$. The x axis indicates the type of ecosystem change adopted and the width of each bar represents the concentration of diversity values.

6 Discussion

Throughout this paper we have explored the ability of different diversity metrics to detect changes in biodiversity beyond stochastic population dynamics. This has involved traditionally used biodiversity measures in ecology and a newly created biodiversity framework. Although there was a great deal of variety in the responses of metrics to different scenarios and habitat types, at least some of the measures were able to reliably detect changes in species abundance and community composition over time. However, the results of these simulation experiments suggest that the ability of metrics to detect consistent trends of biodiversity change depends on both the size and heterogeneity of the habitat.

In particular, we found that most biodiversity metrics were particularly unreliable in terms of both direction and magnitude of response in smaller systems, such as the ‘Patch’ and ‘Island’ habitat types modelled here. Under these conditions, only habitat removal scenarios showed stronger declines in both species richness and abundance, as well as changes in composition. This is of concern to conservation and policy makers,

as smaller refuges such as islands often host unique habitats and endemic species that would not be found elsewhere (Wintle *et al.*, 2019). This lack of signal among the measures is likely due to a larger effect of demographic stochasticity in smaller populations that means it is more difficult to distinguish biodiversity change taking place from that background stochasticity. The observation that smaller community sizes promote greater instability and higher levels of extinction, also known as the small population paradigm, has long been known to metapopulation theory (Caughley, 1994). There is some evidence that in these smaller populations, ecological drift is much stronger so that neutral dynamics are much more likely to govern the system and competition between species is more equal (Orrock & Watling, 2010). In contrast, the larger ‘Region’ and ‘Continent’ systems there is considerably stronger signals in almost all biodiversity metrics and they tend to be more consistent in sign. In these systems, competitive interactions played out more strongly, so that changing as well as removing habitat had an impact on the diversity of the system.

More heterogeneous habitats also produced stronger responses of the biodiversity measures, particularly in regards to the climate warming simulations. Declines in local diversity (alpha) and contribution to overall diversity (gamma) become become more extreme as temperature warming scenarios move from 1 to 3°C. At the same time, local communities became more similar in species composition, so that there was more redundancy (raw rho) and they were more representative of the system as a whole (normalised rho). As temperature warmed in both the gradient and peaked gradient environment, species were forced to move towards cooler climates. During this time, local species extinctions occurred in those that were unable to keep pace with the rate of change, and those that survived had either a preference for warmer climates or a broader range of tolerance to temperature extremes. This change in species composition was detected earliest, even before a loss of local diversity, particularly in the more heterogeneous regions and continents. However, for the homogeneous patches and regions, there was little detection of a change in alpha or gamma diversity at all. Some correlational studies have suggested that alpha diversity is higher or more stable in parts of the world where the rates of climate change are higher (Suggitt *et al.*, 2019). Similarly, analysis of time series data of thousands of taxa across several groups, including fish, mammals, birds and plants, and many different biomes, indicated very little change in many metrics of alpha diversity including species richness (Dornelas *et al.*, 2014).

In order to introduce more realism into the simulations, we also considered environments where the climate fluctuated seasonally. The introduction of this simple oscillation, simulated jointly with various scenarios of temperature increase, completely eliminated the response of any the metrics to climate warming. Here, we consider only a change in the mean temperature that the seasonal cycle oscillates around, but there are many more refinements that could be introduced surrounding the variation and timing of the seasonality (more examples can be found in Waldock *et al.*, 2018). However, even this relatively simplistic scenario throws into doubt our ability to detect changes in biodiversity under more spatially and temporally variable environments.

The detection of changes in beta diversity as a result of habitat loss were seen much earlier and were in general stronger in homogenous and smaller habitats. In contrast to their responses to the temperature increase scenarios, these habitats became more distinctive and therefore less redundant through habitat loss. In these scenarios, habitat is lost immediately with no change to the surrounding habitats, although we know that habitat loss and fragmentation is associated with a general degradation in habitat quality that we do not account for in these models (Hanski, 2011). Therefore, our estimation of the magnitude and timing of biodiversity change are almost certainly underestimates compared to real-life habitat destructive activities, such as deforestation. It is difficult to draw comparisons to prior studies on habitat loss as they are often conducted on small scales (e.g. Fahrig, 2003), and simulations of habitat loss often involve limited numbers of species or plant functional groups, such as those performed by the Madingley model (Bartlett *et al.*, 2016). However, these signals of increased distinctiveness in habitat loss scenarios directly contrasts the increased similarity in species composition that we encountered in the climate change scenarios. There is already some evidence in the literature of increased biotic homogenization as a result of climate change, for example, a study of plants in the Atlantic Forest (Zwiener *et al.*, 2018), and of the converse biotic heterogenization in areas of habitat loss, e.g. deforestation in Brazilian tropical rainforests (Vidal *et al.*, 2019). However, as climate and land-use changes will happen in tandem in some parts of the world, it remains to be seen how effective beta diversity measures would be at detecting changes in species composition given two conflicting drivers such as these.

Although care was taken to parameterise the ecosystems with biologically meaningful values, there is limited information available on demographic rates, dispersal distances and niche preferences for the majority of plant species. In addition to parameterisation, the mechanisms by which demography and competition take place were created to be as general as possible, given the lack of information or focus on any particular plant system. As such, the general terms in the model for resource requirements, niche matching and competition, as well as certain parameters such as λ and τ were derived from many rounds of revision and testing. However, many alternatives exist and can be incorporated in the future, particularly for smaller well-sampled systems where we would be able to fit the models to data. Though we can make general conclusions about the situations in which particular biodiversity metrics performed best, the model is limited in both the complexity of species behaviours and habitat, as well as scenarios of environmental change. Importantly, climate change is expected to have complex and cascading effects on the habitats that could not be captured here by such simplistic interpretations. However, this is an important starting point, as the failure to detect biodiversity change in some measures and change scenarios was evident, even without more complex models. Here, we also assume 100% knowledge of the system to detect changes in biodiversity, even though this is certainly not the case for real life applications of biodiversity measures. There are some intensively sampled plots like the Barro-Colarado Island forest plot (Legendre & Condit, 2019), but for the most part, sampling for plant species across the world is patchy, particularly in the tropics and more inaccessible regions (Corlett, 2016). Further experiments that introduce spatial and taxonomic biases to degrade the data would illuminate further the extent to which

sampling may have affected our interpretation of current biodiversity trends. There is already some evidence that the Reeve *et al.* (2016) diversity framework performs well on sampled populations, depending on the method of sampling used (Mitchell, 2019). Finally, although we included two scenarios of invasive species into the simulation experiments, there was little response for any of the scenarios of habitat types studied. All of the measures used here are naive similarity measures, assuming each species is completely distinct. The inclusion of similarity into the diversity framework is possible (Leinster & Cobbold, 2012), and further investigation is required to see if invasive species with different functional or phylogenetic diversity from native species would be more easily detected.

To date, there have been many correlational studies of temporal changes in biodiversity using sampled data. However, it is extremely difficult to pull apart the contribution of sampling error and demographic stochasticity from different types of pressures (e.g. habitat loss, climate change, invasive species) from the choice of measure, as well as any inherent biases that may exist in the data. Existing simulations exploring the impact on biodiversity of such processes are hindered by either a lack of dynamics (Santini *et al.*, 2016) or limited geographic and taxonomic scope (Hill *et al.*, 2016). The results of this study and the framework we present here for exploring the contribution of different environmental processes to different components of biodiversity change is timely, given the need for both mechanistic, predictive models for future change and for measuring our progress towards revised goals in the Post-2020 Global Biodiversity Framework.

7 Conclusion

In conclusion, here we present a simplified simulation of plant biodiversity that includes demographic and competition processes and can be adapted for both size and type of habitat, as well as simulations of habitat and environmental change. We used this generalisable system of virtual plant communities to explore the effect of several simple scenarios of future change to explore the responses of different biodiversity measures. The ability of the biodiversity measures to detect change beyond the neutral stochastic processes of the system was dependent on both the size and the complexity of the habitat. The impact on biodiversity for smaller ecosystems was more difficult to detect as they underwent more background stochastic change than larger systems. Similarly, more heterogeneous habitat types also responded more strongly and earlier to climate warming scenarios, as local species extinctions occurred in areas that became uninhabitable and species struggled to disperse with the rate of change. More homogeneous habitats, on the other hand, saw earlier and stronger responses to habitat loss scenarios. These results strengthen those from previously published work, in which we saw that no one particular measure could reliably detect changes in biodiversity across all scenarios. Here, the introduction of explicit dynamic processes added a level of stochasticity to the model that often obscured changes in biodiversity, which is particularly concerning when we consider that most biodiversity studies are conducted on smaller

scales in conservation priority areas. Further, the introduction of simplified seasonal fluctuations greatly reduced the responses of the biodiversity metrics across all scenarios of climate change. Although the model is designed here with virtual species, it can be calibrated for more realistic systems and highly complex environmental change processes.

Bibliography

AKÇAKAYA, R. H., BUTCHART, S. H., MACE, G. M., STUART, S. N., & HILTON-TAYLOR, C. (2006). Use and misuse of the IUCN red list criteria in projecting climate change impacts on biodiversity. *Global Change Biology*, **12**(11); pages 2037–2043. ISSN 13541013.

AMTHOR, J. S. (2010). From sunlight to phytomass: On the potential efficiency of converting solar radiation to phyto-energy. *New Phytologist*, **188**(4); pages 939–959. ISSN 0028646X.

BARTLETT, L. J., NEWBOLD, T., PURVES, D. W., TITTENSOR, D. P., & HARFOOT, M. B. J. (2016). Synergistic impacts of habitat loss and fragmentation on model ecosystems. *Proceedings of the Royal Society B: Biological Sciences*, **283**(1839); page 20161,027. ISSN 0962-8452.

BESANÇON, M., ANTHOFF, D., ARSLAN, A., BYRNE, S., LIN, D., PAPAMARKOU, T., & PEARSON, J. (2019). Distributions.jl: Definition and Modeling of Probability Distributions in the JuliaStats Ecosystem.

BEZANSON, J., EDELMAN, A., KARPINSKI, S., & SHAH, V. B. (2017). Julia: A Fresh Approach to Numerical Computing. *SIAM Review*, **59**(1); pages 65–98. ISSN 0036-1445.

BUGMANN, H. (2001). A Review of Forest Gap Models. *Climatic Change*, **51**(3-4); pages 259–305. ISSN 1573-1480.

BULLOCK, J. M., MALLADA GONZILEZ, L., TAMME, R., GÖTZENBERGER, L., WHITE, S. M., PİRTEL, M., & HOOFTMAN, D. A. (2017). A synthesis of empirical plant dispersal kernels. *Journal of Ecology*, **105**(1); pages 6–19. ISSN 13652745.

CASWELL, H. (2001). *Matrix population models: construction, analysis and interpretation*. Sinauer Associates, Sunderland, Massachusetts.

CAUGHLEY, G. (1994). Directions in Conservation Biology. *Journal of Animal Ecology*, **63**(2); pages 215–244.

CHIPPERFIELD, J. D., HOLLAND, E. P., DYTHAM, C., THOMAS, C. D., & HOVESTADT, T. (2011). On the approximation of continuous dispersal kernels in discrete-space models. *Methods in Ecology and Evolution*, **2**(6); pages 668–681. ISSN 2041210X.

CHISHOLM, R. A., CONDIT, R., RAHMAN, K. A., BAKER, P. J., BUNYAVEJCHEWIN, S., CHEN, Y. Y., CHUYONG, G., DATTARAJA, H. S., DAVIES, S., EWANGO, C. E. N., GUNATILLEKE, C. V. S., NIMAL GUNATILLEKE, I. A. U., HUBBELL, S., KENFACK, D., KIRATIPRAYOON, S., LIN, Y., MAKANA, J. R., PONGPATTANANURAK, N., PULLA, S., PUNCHI-MANAGE, R., SUKUMAR, R., SU, S. H., SUN, I. F., SURESH, H. S., TAN, S., THOMAS, D., & YAP, S. (2014). Temporal variability of forest communities: Empirical estimates of population change in 4000 tree species. *Ecology Letters*, **17**(7); pages 855–865. ISSN 14610248.

CLARK, D. B., MERCADO, L. M., HARDING, R. J., ESSERY, R. L. H., SITCH, S., BLYTH, E., ROONEY, G. G., CLARK, D. B., GEDNEY, N., JONES, C. D., HUNTINGFORD, C., BEST, M. J., COX, P. M., BOUCHER, O., & PRYOR, M. (2011). The Joint UK Land Environment Simulator (JULES), model description Part 2: Carbon fluxes and vegetation dynamics. *Geoscientific Model Development*, **4**(3); pages 701–722. ISSN 1991-9603.

CLARK, J. S., SILMAN, M., KERN, R., MACKLIN, E., & HILLERISLAMBERS, J. (1999). Seed Dispersal Near And Far: Patterns Across Temperatue And Tropical Forests. *Ecology*, **80**(5); pages 1475–1494.

CONNELL, J. H. (1978). Diversity in Tropical Rain Forests and Coral Reefs. *Science*, **199**(4335); pages 1302–1310. ISSN 0012-9623.

CORLETT, R. T. (2016). Plant diversity in a changing world: Status, trends, and conservation needs. *Plant Diversity*, **38**(1); pages 10–16. ISSN 24682659.

Cox, P. M. (2001). Description of the "TRIFFID" Dynamic Global Vegetation Model.

DE BLASIO, F. V., LIOW, L. H., SCHWEDER, T., & DE BLASIO, B. F. (2015). A model for global diversity in response to temperature change over geological time scales, with reference to planktic organisms. *Journal of Theoretical Biology*, **365**; pages 445–456. ISSN 10958541.

DORNELAS, M. (2010). Disturbance and change in biodiversity. *Philosophical Transactions of the Royal Society B: Biological Sciences*, **365**(1558); pages 3719–3727. ISSN 0962-8436.

DORNELAS, M., GOTELLI, N. J., MCGILL, B., SHIMADZU, H., MOYES, F., SIEVERS, C., & MAGURRAN, A. E. (2014). Assemblage Time Series Reveal Biodiversity Change but Not Systematic Loss. *Science*, **344**(6181); pages 296–299. ISSN 0036-8075.

ENGLER, R. & GUISAN, A. (2009). MigClim: Predicting plant distribution and dispersal in a changing climate. *Diversity and Distributions*, **15**(4); pages 590–601. ISSN 13669516.

FAHRIG, L. (2003). Effects of Habitat Fragmentation on Biodiversity. *Annual Review of Ecology, Evolution, and Systematics*, **34**(1); pages 487–515. ISSN 1543-592X.

FAITH, D. P. (1992). Conservation evaluation and phylogenetic diversity. *Biological Conservation*, **61**; pages 1–10. ISSN 00063207.

FICK, S. E. & HIJMANS, R. J. (2017). WorldClim 2: new 1-km spatial resolution climate surfaces for global land areas. *International Journal of Climatology*, **37**(12); pages 4302–4315. ISSN 10970088.

FISCHER, R., BOHN, F., DANTAS DE PAULA, M., DISLICH, C., GROENEVELD, J., GUTIÉRREZ, A. G., KAZMIERCZAK, M., KNAPP, N., LEHMANN, S., PAULICK, S., PÜTZ, S., RÖDIG, E., TAUBERT, F., KÖHLER, P., & HUTH, A. (2016). Lessons learned from applying a forest gap model to understand ecosystem and carbon dynamics of complex tropical forests. *Ecological Modelling*, **326**; pages 124–133. ISSN 03043800.

GOOD, S. P., MOORE, G. W., & MIRALLES, D. G. (2017). A mesic maximum in biological water use demarcates biome sensitivity to aridity shifts. *Nature Ecology and Evolution*, **1**(12); pages 1883–1888. ISSN 2397334X.

GRIME, J. P. (1973). Competitive Exclusion in Herbaceous Vegetation. *Nature*, **242**(1); pages 344–347.

HANNAH, L. (2014). Modeling Species and Ecosystem Response. *Climate Change Biology*, pages 237–262.

HANSKI, I. (2011). Habitat Loss, the Dynamics of Biodiversity, and a Perspective on Conservation. *AMBIO*, **40**(3); pages 248–255. ISSN 0044-7447.

HARFOOT, M. B. J., NEWBOLD, T., TITTENSOR, D. P., EMMOTT, S., HUTTON, J., LYUTSAREV, V., SMITH, M. J., SCHARLEMANN, J. P. W., & PURVES, D. W. (2014). Emergent Global Patterns of Ecosystem Structure and Function from a Mechanistic General Ecosystem Model. *PLoS Biology*, **12**(4). ISSN 15457885.

HARPER, A. B., COX, P. M., FRIEDLINGSTEIN, P., WILTSHERE, A. J., JONES, C. D., SITCH, S., MERCADO, L. M., GROENENDIJK, M., ROBERTSON, E., KATTGE, J., BÖNISCH, G., ATKIN, O. K., BAHN, M., CORNELISSEN, J., NIINEMETS, Ü., ONIPCHENKO, V., PEÑUELAS, J., POORTER, L., REICH, P. B., SOUDZILOVSKAIA, N. A., & VAN BODEGOM, P. (2016). Improved representation of plant functional types and physiology in the Joint UK Land Environment Simulator (JULES v4.2) using plant trait information. *Geoscientific Model Development*, **9**(7); pages 2415–2440. ISSN 19919603.

HARTE, J. & NEWMAN, E. A. (2014). Maximum information entropy: A foundation for ecological theory. *Trends in Ecology and Evolution*, **29**(7); pages 384–389. ISSN 01695347.

HILL, M. O. (1973). Diversity and Evenness: A Unifying Notation and Its Consequences. *Ecology*, **54**(2); pages 427–432. ISSN 00129658.

HILL, S. L., HARFOOT, M., PURVIS, A., PURVES, D. W., COLLEN, B., NEWBOLD, T., BURGESS, N. D., & MACE, G. M. (2016). Reconciling Biodiversity Indicators to Guide Understanding and Action. *Conservation Letters*, **9**(6); pages 405–412. ISSN 1755263X.

HUBBELL, S. (1979). Tree dispersion, abundance, and diversity in a tropical dry forest. *Science*, **203**(4387); pages 1299–1309. ISSN 0036-8075.

HUBBELL, S. P. (2001). *The Unified Neutral Theory of Biodiversity and Biogeography*. Princeton University Press. ISBN 9780691021287.

INTERGOVERNMENTAL PANEL ON CLIMATE CHANGE (2018). IPCC, 2018: Summary for Policymakers. In MASSON-DELMOTTE, V., ZHAI, P., PORTNER, H.-O., ROBERTS, D., SKEA, J., SHUKLA, P., PIRANI, A., MOUFOUMA-OKIA, W., PEAN, C., PIDCOCK, R., CONNORS, S., MATTHEWS, J., CHEN, Y., ZHOU, X., GOMIS, M., LONNOY, E., MAYCOCK, T., TIGNOR, M., & WATERFIELD, T., editors, *Global Warming of 1.5C. An IPCC Special Report on the impacts of global warming of 1.5C above pre-industrial levels and related global greenhouse gas emission pathways, in the context of strengthening the global response to the threat of climate change*,, pages 1–32. World Meteorological Organization.

KEITH, D. A., AKÇAKAYA, H. R., THUILLER, W., MIDGLEY, G. F., PEARSON, R. G., PHILLIPS, S. J., REGAN, H. M., ARAÚJO, M. B., & REBELO, T. G. (2008). Predicting extinction risks under climate change: Coupling stochastic population models with dynamic bioclimatic habitat models. *Biology Letters*, **4**(5); pages 560–563. ISSN 1744957X.

LEGENDRE, P. & CONDIT, R. (2019). Spatial and temporal analysis of beta diversity in the Barro Colorado Island forest dynamics plot, Panama. *Forest Ecosystems*, **6**(1); page 7. ISSN 2197-5620.

LEINSTER, T. & COBBOLD, C. A. (2012). Measuring diversity: The importance of species similarity. *Ecology*, **93**(3); pages 477–489. ISSN 00129658.

LEXER, M. J. & HÖNNINGER, K. (2001). A modified 3D-patch model for spatially explicit simulation of vegetation composition in heterogeneous landscapes. *Forest Ecology and Management*, **144**(1-3); pages 43–65. ISSN 03781127.

MARBA, N., DUARTE, C. M., & AGUSTI, S. (2007). Allometric scaling of plant life history. *Proceedings of the National Academy of Sciences*, **104**(40); pages 15,777–15,780. ISSN 0027-8424.

MELBOURNE, B. A. (2012). Demographic stochasticity. In HASTINGS, A. & GROSS, L. J., editors, *Encyclopedia of Theoretical Ecology*, pages 706–712. University of California Press, Berkeley.

MITCHELL, S. (2019). *The measurement, dynamics, and interpretation of biological diversity*. Ph.D. thesis, University of Glasgow.

MOORCROFT, P. R., HURTT, G. C., & PACALA, S. W. (2001). A Method for Scaling Vegetation Dynamics: the Ecosystem Demography Model (Ed). *Ecological Monographs*, **71**(4); pages 557–586. ISSN 0012-9615.

ORROCK, J. L. & WATLING, J. I. (2010). Local Community size mediates ecological drift and competition in metacommunities. *Proceedings of the Royal Society B: Biological Sciences*, **277**(1691); pages 2185–2191. ISSN 14712970.

PEARSON, R. G. & DAWSON, T. P. (2003). Predicting the impacts of climate change on the distribution of species: are bioclimate envelope models useful? *Global Ecology and Biogeography*, **12**(5); pages 361–371. ISSN 1466-822X.

PURVES, D., SCHARLEMANN, J. P. W., HARFOOT, M., NEWBOLD, T., TITTENSOR, D. P., HUTTON, J. M., & EMMOTT, S. (2013). Time to model all life on Earth. *Nature*, **493**(7432); pages 295–297. ISSN 1476-4687.

QUILLET, A., PENG, C., & GARNEAU, M. (2010). Toward dynamic global vegetation models for simulating vegetationclimate interactions and feedbacks: recent developments, limitations, and future challenges. *Environmental Reviews*, **18**; pages 333–353. ISSN 1181-8700.

REEVE, R., MITCHELL, S. N., LEINSTER, T., COBBOLD, C. A., THOMPSON, J., BRUMMITT, N., MATHER, A. E., BROWN, D. J., COIA, J. E., & MATTHEWS, L. (2016). How to partition diversity. *In prep.*

REICH, P. B. (2001). Body size, geometry, longevity and metabolism: do plant leaves behave like animal bodies? *Trends in Ecology and Evolution*, **16**(12); pages 674–680. ISSN 01695347.

SANTINI, L., BELMAKER, J., COSTELLO, M. J., PEREIRA, H. M., ROSSBERG, A. G., SCHIPPER, A. M., CEAUSU, S., DORNELAS, M., HILBERS, J. P., HORTAL, J., HUIJBREGTS, M. A. J., NAVARRO, L. M., SCHIFFERS, K. H., VISCONTI, P., & RONDININI, C. (2016). Assessing the suitability of diversity metrics to detect biodiversity change. *Biological Conservation*, pages 1–10. ISSN 00063207.

SHANNON, C. E. (1948). A mathematical theory of communication. *The Bell System Technical Journal*, **27**; pages 379–423. ISSN 07246811.

SHUGART, H. H., WANG, B., FISCHER, R., MA, J., FANG, J., YAN, X., HUTH, A., & ARMSTRONG, A. H. (2018). Gap models and their individual-based relatives in the assessment of the consequences of global change. *Environmental Research Letters*, **13**(3). ISSN 17489326.

SIMPSON, E. H. (1949). Measurement of Diversity.

SØRENSEN, T. (1948). A Method of Establishing Groups of Equal Amplitude in Plant Sociology Based on Similarity of Species Content and its Application to Analyses of the Vegetation on Danish Commons. *Det Kongelige Danske Videnskabernes Selskab Biologiske Skrifter*, **5**; pages 1–34. ISSN 0001-6926.

SUGGITT, A. J., LISTER, D. G., & THOMAS, C. D. (2019). Widespread Effects of Climate Change on Local Plant Diversity. Technical report.

THOMSON, F. J., MOLES, A. T., AULD, T. D., & KINGSFORD, R. T. (2011). Seed dispersal distance is more strongly correlated with plant height than with seed mass. *Journal of Ecology*, **99**(6); pages 1299–1307. ISSN 00220477.

THUILLER, W., ALBERT, C., ARAÚJO, M. B., BERRY, P. M., CABEZA, M., GUISAN, A., HICKLER, T., MIDGLEY, G. F., PATERSON, J., SCHURR, F. M., SYKES, M. T., & ZIMMERMANN, N. E. (2008). Predicting global change impacts on plant species' distributions: Future challenges. *Perspectives in Plant Ecology, Evolution and Systematics*, **9**(3-4); pages 137–152. ISSN 16180437.

URBAN, M. C., BOCEDI, G., HENDRY, A. P., MIHOUB, J.-B., PEER, G., SINGER, A., BRIDLE, J. R., CROZIER, L. G., DE MEESTER, L., GODSOE, W., GONZALEZ, A., HELLMANN, J. J., HOLT, R. D., HUTH, A., JOHST, K., KRUG, C. B., LEADLEY, P. W., PALMER, S. C. F., PANTEL, J. H., SCHMITZ, A., ZOLLNER, P. A., & TRAVIS, J. M. J. (2016). Improving the forecast for biodiversity under climate change. *Science*, **353**(6304); pages aad8466–aad8466. ISSN 0036-8075.

VIDAL, C. Y., ROCHA, D. S. B., DE SIQUEIRA, M. F., RODRIGUES, R. R., & SIQUEIRA, T. (2019). Heterogenization of remaining biodiversity in fragmented tropical forests across agricultural landscapes. *In prep.* ISSN 0044-4642.

WALDOCK, C., DORNELAS, M., & BATES, A. E. (2018). Temperature-Driven Biodiversity Change: Disentangling Space and Time. *BioScience*, **68**(11); pages 873–884. ISSN 0006-3568.

WINTLE, B. A., KUJALA, H., WHITEHEAD, A., CAMERON, A., VELOZ, S., KUKKALA, A., MOILANEN, A., GORDON, A., LENTINI, P. E., CADENHEAD, N. C. R., & BEKESSY, S. A. (2019). Global synthesis of conservation studies reveals the importance of small habitat patches for biodiversity. *Proceedings of the National Academy of Sciences*, **116**(3); pages 909–914. ISSN 0027-8424.

ZWIENER, V. P., LIRA-NORIEGA, A., GRADY, C. J., PADIAL, A. A., & VITULE, J. R. (2018). Climate change as a driver of biotic homogenization of woody plants in the Atlantic Forest. *Global Ecology and Biogeography*, **27**(3); pages 298–309. ISSN 14668238.